Published for SISSA by Springer
Received: September 1, 2017
Revised: November 14, 2017
Accepted: November 25, 2017
Published: December 14, 2017

Collectivity from interference

Boris Blok,[a] **Christian D. Jäkel,**[b] **Mark Strikman**[c] **and Urs Achim Wiedemann**[d]

[a] *Department of Physics, Technion — Israel Institute of Technology, Haifa 3200003, Israel*
[b] *Department of Applied Mathematics, University of São Paulo (USP), CEP 05508-090, São Paulo, Brazil*
[c] *Department of Physics, Penn State University, 104 Davey Lab, University Park, PA 16802-6300, U.S.A.*
[d] *Theoretical Physics Department, CERN, CH-1211 Genève 23, Switzerland*

E-mail: blok@ph.technion.ac.il, jaekel@ime.usp.br, mxs43@psu.edu, urs.wiedemann@cern.ch

Abstract: In hadronic collisions, interference between different production channels affects momentum distributions of multi-particle final states. As this QCD interference does not depend on the strong coupling constant α_s, it is part of the no-interaction baseline that needs to be controlled prior to searching for other manifestations of collective dynamics, e.g., in the analysis of azimuthal anisostropy coefficients v_n at the LHC. Here, we introduce a model that is based on the QCD theory of multi-parton interactions and that allows one to study interference effects in the production of m particles in hadronic collisions with N parton-parton interactions ("sources"). In an expansion in powers of $1/(N_c^2-1)$ and to leading order in the number of sources N, we calculate interference effects in the m-particle spectra and we determine from them the second and fourth order cumulant momentum anisotropies $v_n\{2\}$ and $v_n\{4\}$. Without invoking any azimuthal asymmetry and any density dependent non-linear dynamics in the incoming state, and without invoking any interaction in the final state, we find that QCD interference alone can give rise to values for $v_n\{2\}$ and $v_n\{4\}$, n even, that persist unattenuated for increasing number of sources, that may increase with increasing multiplicity and that agree with measurements in proton-proton (pp) collisions in terms of the order of magnitude of the signal and the approximate shape of the transverse momentum dependence. We further find that the non-abelian features of QCD interference can give rise to odd harmonic anisotropies. These findings indicate that the no-interaction baseline including QCD interference effects can make a sizeable if not dominant contribution to the measured v_n coefficients in pp collisions. Prospects for analyzing QCD interference contributions further and their possible relevance for proton-nucleus and nucleus-nucleus collisions are discussed shortly.

Keywords: Heavy Ion Phenomenology

ArXiv ePrint: 1708.08241

https://doi.org/10.1007/JHEP12(2017)074

JHEP12(2017)074

Contents

JHEP12(2017)074

1 Introduction

Multi-particle production in proton-proton (pp) collisions is typically modeled in terms of multiple parton-parton interactions without invoking explicitly density-dependent dynamics in the incoming wave functions or final state rescattering of the outgoing partons. In particular, multi-purpose event generators provide a reasonable modeling of many characteristics of the underlying event in proton-proton collisions [1–4], but the simulation of effects that relate different parton-parton interactions is largely limited to ensuring consequences of global conservation laws (energy, momentum, color). The standard picture of multi-particle production in ultra-relativistic nucleus-nucleus (AA) collisions is radically different. Here, jet quenching provides unambiguous evidence for significant final state rescattering effects [5–7]. Rescattering is a precursor of fluid dynamics. Partonic systems in which rescattering is operational can be described by an effective kinetic theory that is known to hydrodynamize rapidly [8]. Indeed, fluid dynamical modeling has been demonstrated to provide a phenomenologically valid basis for the simulation of soft multi-particle production in heavy ion collisions [9].

The different dynamical pictures of multi-particle production in pp, pA and AA may be mutually compatible. The transverse size of the systems produced in pp collisions may be sufficiently small for rescattering effects to be negligible, while pA and AA collisions may be sufficiently large and dense to be dominated by multiple rescattering in the final state. However, the recent observation of heavy-ion like behavior in pp (and pA) collisions at the LHC challenges this simple interpretation. On the one hand, the observation of a strong multiplicity-dependence of (multi-)strange hadron production in pp collisions [10] and of momentum anisotropies in pp and pA collisions [11–14] seems incompatible with modeling such collisions as an essentially incoherent superposition of multiple partonic interactions supplemented by global constraints (see, e.g., refs. [15–18] for attempts to model these phenomena). On the other hand, the apparent absence of rescattering effects in inclusive jet and hadron production (above $p_T \sim O(1\,\mathrm{GeV})$) in pp and pA [19–21] raises the question whether final state rescattering is sufficiently effective in the smaller collision systems to give rise to measurable signs of collectivity.

This prompts us to ask whether physical phenomena could be at work that contribute to the recent observations of heavy-ion like behavior in pp collisions without invoking final state rescattering or density dependent dynamics in the incoming state. Our focus will be on QCD interference effects, as these do not depend on the coupling constant α_s or on interaction probability while they are known to affect multi-particle distributions in the final state. We are mainly interested in understanding their contribution to the anisotropy coefficients $v_m\{2n\}$ that are measured in pp, pPb and PbPb collisions from connected $(2n)$-particle correlation functions via the so-called cumulant technique [22–24]. QCD interference is known to lead to momentum anisotropies in the 2-particle cumulant $v_2\{2\}$ (for a rederivation, see section 3 below). However, also the measured higher order cumulants $v_m\{2n\}$ show the same p_T-, rapidity- and multiplicity-dependent sizeable values (that are typically 20% smaller than $v_m\{2\}$). This is commonly refered to as a signature of collectivity [11, 12], since it is consistent with a correlation amongst all particles in the event.

JHEP12(2017)074

The technical question that we shall address with explicit calculations in this manuscript is whether QCD interference can give rise to non-vanishing higher order cumulants $v_m\{2n\}$ and how these are expected to scale with system size.

Under the assumption that hadronic wave functions at ultra-relativistic energies carry saturated gluon distributions, multi-particle correlations have been calculated in the so-called CGC-formalism [25–39]. This formalism combines effects that are non-negotiably at work (i.e., QCD interference) with effects of a saturated gluon distribution that are searched for as signatures of QCD in a novel high-density regime. In contrast, we work in a simplified model that treats QCD interference exactly but that does not invoke parton saturation effects. This may ultimately help to disentangle both classes of effects. In section 2, we define a QCD-inspired model of multi-particle production that is sufficiently simple to allow for explicit calculations of higher order cumulants. In sections 3 and 4, we calculate v_2 from 2-, 4- and 6-particle cumulants, before summarizing our preliminary analysis of odd harmonics in section 5. Section 6 discusses how the model defined in section 2 is related to the theory of multi-parton interactions. This allows us to estimate the value of the only model parameter, which we use in section 7 to obtain some numerical results. We conclude by summarizing the main conclusions as well as important open questions.

2 A model of multi-particle production

2.1 Defining the model

The model for multi-particle production introduced here views a hadronic collision as an event consisting of N parton-parton interactions occurring at positions $\mathbf{y}_i$, $i \in [1, N]$, in the transverse plane. To each of the transverse positions $\mathbf{y}_i$, the model associates a partonic line source which may be thought of as starting with initial color b_i at the rapidity of the first colliding hadron, emitting gluons in the intermediate rapidity window and ending at the rapidity of the second hadron with final color c_i. Each multi-particle production amplitude is therefore of the type given in figure 1. The model can be summarized as follows:

1. Each hadron collision is characterized by a set $\{\mathbf{y}_i, b_i\}$, $i \in [1, N]$, of N particle emitting sources distributed at transverse positions $\mathbf{y}_i$ with initial colors b_i in the adjoint representation.

2. Gluon emission from a source at position $\mathbf{y}_j$ and color b_j is described by an eikonal vertex,

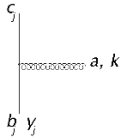

$$= T^a_{b_j c_j} \int d\mathbf{x}\, \vec{f}(\mathbf{x}-\mathbf{y})\, e^{i\,\mathbf{k}.\mathbf{x}} \equiv T^a_{b_j c_j}\, \vec{f}(\mathbf{k})\, \exp\left[i\,\mathbf{y}.\mathbf{k}\right] , \qquad (2.1)$$

where the integration variable $\mathbf{x}$ is two-dimensional transverse, and the color structure of the vertex is defined by the adjoint generators T^a of $\mathrm{SU}(N_c)$. The vertex function $\vec{f}$ is a two-dimensional vector in the transverse plane, that in cross sections will appear

JHEP12(2017)074

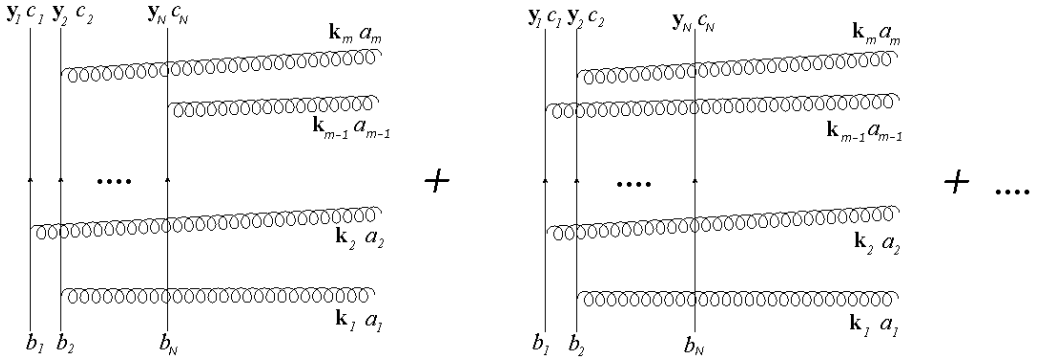

Figure 1. Two of the N^m diagrammatic contribution to the m-gluon emission amplitude from N sources. The N partonic line sources in adjoint representation start with initial colors b_j and, after emitting gluons, end at final color c_j. Emitted gluons are regarded as being ordered in rapidity, see text for details.

dotted into another vertex function. For instance, for gluons in the non-abelian Coulomb field of an incoming source, one may write $\vec{f}(\mathbf{k}) \propto g\mathbf{k}/\mathbf{k}^2$. In the following calculations, however, we do not assume a specific functional shape of $\vec{f}(\mathbf{k})$. The vector $\vec{f}(\mathbf{k})$ parametrizes then the $\mathbf{k}$-dependent microscopic dynamics that gives rise to gluon emission.

3. When calculating cross sections of event samples, the initial data are weighted with a *classical* probability distribution $\rho\,(\{\mathbf{y}_i\})$. Denoting coordinates in the complex conjugate amplitude with primes, this means that initial data $\{\mathbf{y}_i, b_i\}$ and $\{\mathbf{y'}_i, b'_i\}$ are averaged with the weight $\rho\,(\{\mathbf{y}_i\})\ \delta^{(2)}\,(\mathbf{y}_i - \mathbf{y'}_i)\ \delta_{b_i,b'_i}$. Also, final colors are summed over with the constraint δ_{c_i,c'_i}.

According to the model defined above, the spectrum for emission of m particles of transverse momenta $\mathbf{k}_1, \ldots, \mathbf{k}_m$ from N sources takes the form

$$\frac{d\Sigma}{d\mathbf{k}_1 \ldots d\mathbf{k}_m} = \int \left(\prod_{i=1}^{N} d\mathbf{y}_i \right) \rho(\{y_i\})\, \hat{\sigma}\,(\{\mathbf{k}_j\}, \{y_i\})\ . \tag{2.2}$$

Here, $\hat{\sigma}(\{\mathbf{k}_j\}, \{\mathbf{y_i}\})$ denotes the spectrum for the production of m particles of momentum $\{\mathbf{k}_j\}$, $j \in [1, m]$ from N sources at specific positions $\{\mathbf{y_i}\})$, $i \in [1, N]$. Phenomenologically relevant values for m and N may be fixed by noting that high-multiplicity proton-proton collisions at the LHC can contain $m \sim O(100)$ particles, and events of this multiplicity are modeled in Monte Carlo event generators typically with $N \sim O(10)$ parton-parton interactions. However, the main focus of the present work is not on this phenomenologically relevant parameter range but on the qualitative question of whether QCD interference can give rise to momentum anisotropies v_n that persist in higher order cumulants. To this end, the main aim of this manuscript is to calculate $\hat{\sigma}\,(\{\mathbf{k}_j\}, \{y_i\})$ for arbitrary values of m and N, and to analyze in particular the limit of large N in which possible asymmetries due to fluctuations in the number of sources are absent. We do this with the following simplifications:

JHEP12(2017)074

1. *Neglecting longitudinal phase factors.* Only transverse momenta and transverse coordinates are considered explicitly in the model. The rationale for this simplification is the following: one could supplement the model with longitudinal phase factors in the definition of the vertex function (2.1) by replacing $\vec{f}(\mathbf{x}-\mathbf{y})\, e^{i\,\mathbf{k}.\mathbf{x}} \longrightarrow \vec{f}(x-y)\, e^{i\,\mathbf{k}.\mathbf{x}} e^{i\,k^+x^- + i\,k^-x^+}$, where the indices $\pm$ denote components of light-cone coordinates and momenta. For high collision energy, however, when both the emitting sources and the emitted gluons propagate close to the light cone, one has $k^- \approx 0$. This implies that $e^{i\,k^-x^+} \approx 1$.

   If the remaining phase $e^{i\,k^+x^-}$ were included in the following calculations of gluon production cross sections, it would result in an additional multiplicative factor $e^{i\,k^+(y_i-y_j)^-}$ in those terms in which a factor $e^{i\,\mathbf{k}.(\mathbf{y}_i-\mathbf{y}_j)}$ occurs. Here, y_i, y_j denote generic positions of sources from which the gluon of momentum k is emitted in the amplitude and absorbed in the complex conjugate amplitude, respectively. However, identifying the particle emitting source with an energetic parton of light cone momentum fraction p_i^+, it follows from the uncertainty relation that $y_i^- \sim 1/p_i^+$. For soft emitted gluons ($k^+ \ll p_i^+$), this phase is hence negligible, too, $k^+(y_i-y_j)^- \sim \frac{k^+}{p_i^+} - \frac{k^+}{p_j^+} \ll 1$.

   We therefore conclude that longitudinal dynamics can be neglected when discussing phase interference. After a first illustrative calculation, we shall explain at the end of section 3.1 why gluons are correlated in transverse momentum even if they are separated by a significant rapidity interval.

2. *Emitted gluons do not cross.* In several simpler examples, it was demonstrated explicitly that contributions to the multi-gluon cross section of maximal power in $\ln(1/x)$ arise in light cone gauge from ladder diagrams in which emissions are strongly ordered in rapidity, see e.g. [40]. It is not known how these arguments extend to the more complex problem of radiation of many soft gluons from multiple sources discussed here. However, our aim is to devise a model that retains relevant features of QCD but that is simple enough to allow for the explicit calculation of soft multi-gluon interference for large m and N. Motivated by the above-mentioned results for multi-gluon cross sections in simpler systems and by the need for computational simplicity, we therefore assume that multi-gluon radiation is dominated by ladder-type diagrams in which gluon lines do not cross, and we think of the emitted gluons as ordered in rapidity.

3. *m-particle emission cross sections will be symmetrized amongst the m emittees.* We shall find that interference contributions to multi-particle emission cross sections are not always symmetric under interchange between final state momenta $\mathbf{k}_i$. This is so, since the color constraints on gluon emission of the first ($i = 1, 2 \ldots$) and last ($i = \ldots, m-1, m$) gluons in the emission amplitude are different from those in between, see appendices A and B for technical details. As these differences are small and unimportant for our discussion, but since they lead to much longer expressions for higher order cumulants, we shall often randomize final results by averaging over

JHEP12(2017)074

all permutations s of the m outgoing momenta,

$$\frac{d\Sigma}{d\mathbf{k}_1 \dots d\mathbf{k}_m} \longrightarrow \frac{1}{m!} \sum_s \frac{d\Sigma}{d\mathbf{k}_{s(1)} \dots d\mathbf{k}_{s(m)}} \,. \tag{2.3}$$

4. *No modelling of hadronization.* Throughout this work, we calculate *partonic* spectra and momentum correlations. If hadronization would satisfy local parton-hadron duality (LPHD), then our result could be compared to measured hadron spectra and correlations. However, the simple LPHD prescription may not be phenomenologically viable for multi-particle correlations at soft transverse momentum. We regard it as a limitation of this work that we do not address uncertainties arising from the hadronization stage. We emphasize that our main focus is on addressing the *qualitative* question of whether QCD interference can give rise to momentum anisotropies v_n that persist in higher order cumulants. Since any valid hadronization prescription conserves momentum flow in azimuth, the qualitative answer to this question should not depend on details of the hadronization model, and realistic hadronization models are expected to preserve the order of magnitude of the azimuthal asymmetries found on the partonic level. However, hadronic particle spectra and correlations are generally softened and smeared compared to their partonic parents. This is in particular a caveat for the interpretation of the transverse momentum dependencies of azimuthal anisotropy coefficient v_n discussed in section 7.

2.2 Azimuthal multi-particle correlations

To define two-particle correlation functions, we average the m-particle emission spectrum in (2.2) with a phase factor $e^{in(\phi_1-\phi_2)}$,

$$T_n(k_1,k_2) = \binom{m}{2} \int_\rho \int_0^{2\pi} d\phi_1\, d\phi_2\, \exp\left[in(\phi_1-\phi_2)\right] \left(\int \prod_{b=3}^{m} k_b\, dk_b\, d\phi_b \right) \hat{\sigma}\,, \tag{2.4}$$

where k_i, ϕ_i denote the radial and azimuthal components of the two-dimensional transverse momenta $\mathbf{k}_i$. We also construct the corresponding norm

$$\overline{T}(k_1,k_2) = \binom{m}{2} \int_\rho \int_0^{2\pi} d\phi_1\, d\phi_2 \left(\int \prod_{b=3}^{m} k_b\, dk_b\, d\phi_b \right) \hat{\sigma}\,, \tag{2.5}$$

where the Binomial coefficient $\binom{m}{2}$ counts the number of particle pairs in an event. The integration $\int_\rho \dots \equiv \int \left(\prod_{i=1}^{N} d\mathbf{y}_i\right) \rho(\{y_i\}) \dots$ amounts to an average for a specific event sample that is defined by the source distribution ρ. The angular two-particle correlation function $\langle\langle e^{in(\phi_1-\phi_2)}\rangle\rangle$ is then defined as [23, 24]

$$\langle\langle e^{in(\phi_1-\phi_2)}\rangle\rangle(k_1,k_2) \equiv \frac{T_n(k_1,k_2)}{\overline{T}(k_1,k_2)} \,. \tag{2.6}$$

The experimentally measured (second-order cumulant) anisotropy coefficients $v_n^2\{2\}$ can be identified with (2.6),

$$v_n^2\{2\}(k_1,k_2) \equiv \langle\langle e^{in(\phi_1-\phi_2)}\rangle\rangle(k_1,k_2)\,. \tag{2.7}$$

JHEP12(2017)074

We follow experimental practice by defining

$$v_n\{2\}(k) \equiv \sqrt{\langle\langle e^{in(\phi_1-\phi_2)}\rangle\rangle(k,k)}\,. \tag{2.8}$$

However, (2.7) cannot be expected to factorize, and in general $\langle\langle e^{in(\phi_1-\phi_2)}\rangle\rangle(k_1,k_2) \neq v_n\{2\}(k_1)\,v_n\{2\}(k_2)$ (see sections 4.1 and 7).

Correlation functions for more than 2 particles can be defined analogously [23, 24]. In particular, we shall calculate the normalized azimuthal 4-particle correlation functions $\langle\langle e^{in(\phi_1+\phi_2-\phi_3-\phi_4)}\rangle\rangle$ from

$$S_n(k_1,k_2,k_3,k_4) = \binom{m}{4}\int_\rho\int_0^{2\pi} d\phi_1\,d\phi_2\,d\phi_3\,d\phi_4\,e^{in(\phi_1+\phi_2-\phi_3-\phi_4)}\left(\int\prod_{b=5}^{m}k_b\,dk_b\,d\phi_b\right)\hat{\sigma}\,, \tag{2.9}$$

and from the corresponding normalization $\overline{S}$ obtained by evaluating (2.9) without phase factors. The fourth order cumulants are then defined in the standard way,

$$\begin{aligned}\langle\langle e^{in(\phi_1+\phi_2-\phi_3-\phi_4)}\rangle\rangle_c &= \langle\langle e^{in(\phi_1+\phi_2-\phi_3-\phi_4)}\rangle\rangle \\ &\quad - \langle\langle e^{in(\phi_1-\phi_3)}\rangle\rangle\langle\langle e^{in(\phi_2-\phi_4)}\rangle\rangle - \langle\langle e^{in(\phi_1-\phi_4)}\rangle\rangle\langle\langle e^{in(\phi_2-\phi_3)}\rangle\rangle\,,\end{aligned} \tag{2.10}$$

which defines the fourth order cumulant anisotropy coefficient

$$v_n\{4\} \equiv \sqrt[4]{-\langle\langle e^{in(\phi_1+\phi_2-\phi_3-\phi_4)}\rangle\rangle_c}\,. \tag{2.11}$$

3 The dipole interference term

3.1 Explicit calculation of a simple example: $N = 2$, $m = 2$

To illustrate the calculation of the spectrum $\hat{\sigma}$ in (2.2), we discuss now the case of emitting $m = 2$ gluons from $N = 2$ sources. Figure 2 shows the 16 diagrammatic contributions. The first row of figure 2 shows *diagonal* contributions in which all gluons are emitted from the same source in the amplitude and in the complex conjugate amplitude. These contributions are free of interference effects. Denoting by a and b the colors of the two emitted gluons, we find for the top left and top right diagrams the color factor (we work in the adjoint representation)

$$\mathrm{Tr}\left[T^aT^bT^bT^a\right]\mathrm{Tr}\left[\mathbb{1}\right] = N_c^2\left(N_c^2-1\right)^2\,. \tag{3.1}$$

The second and third diagrams on the top row of figure 2 have the color factor $\mathrm{Tr}\left[T^aT^a\right]\mathrm{Tr}\left[T^bT^b\right] = N_c^2\left(N_c^2-1\right)^2$, so that all diagrams on the top row of figure 2 have the same color factor (3.1).

The second row of figure 2 shows the four diagrammatic contributions for which both emitted gluons are *off-diagonal*, i.e., they are emitted from one source in the amplitude and they are absorbed by the other source in the complex conjugate amplitude. The corresponding color factor reads

$$\mathrm{Tr}\left[T^aT^b\right]\mathrm{Tr}\left[T^bT^a\right] = N_c^2\left(N_c^2-1\right)\,. \tag{3.2}$$

JHEP12(2017)074

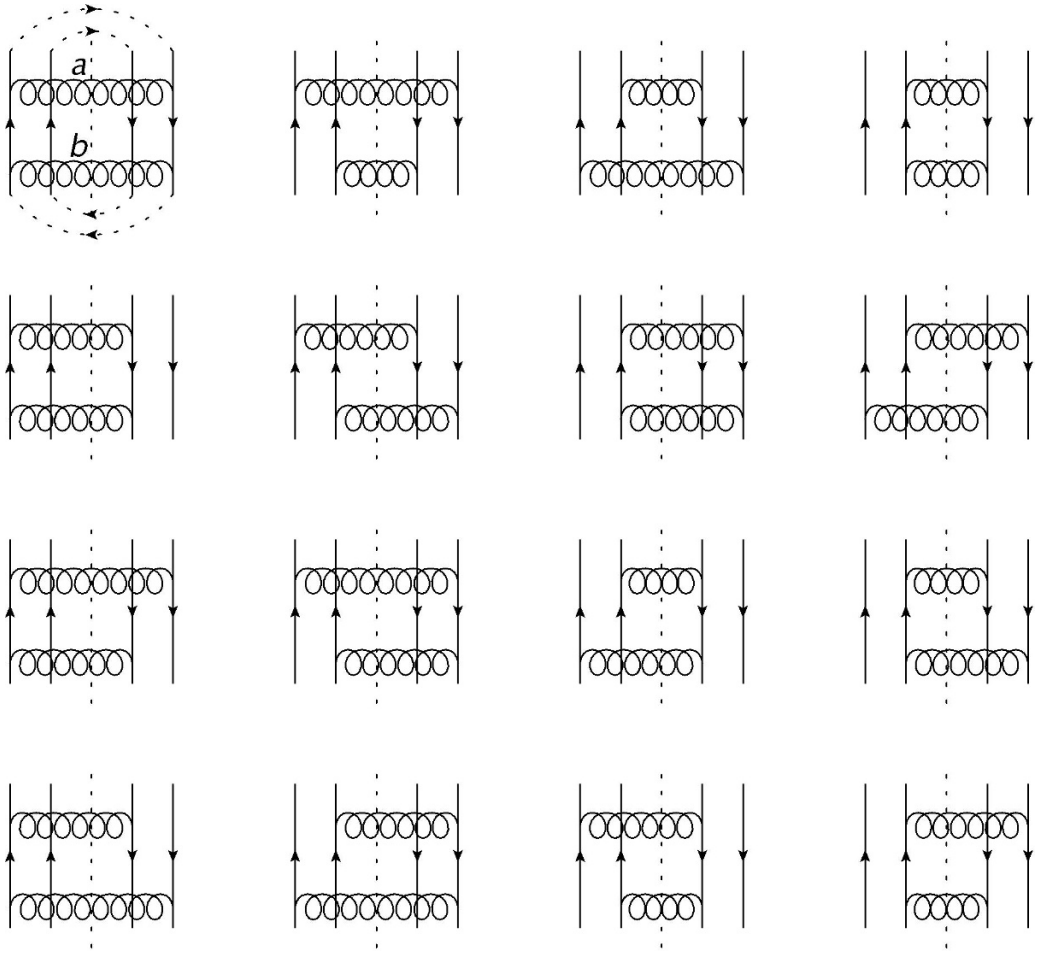

Figure 2. The 16 diagrammatic contributions to the 2-gluon emission spectrum from 2 sources. In each of the 16 diagrams, contributions from the amplitude (complex conjugate amplitude) are on the left (right) hand side of the dotted line. Averaging (summing) over the initial (final) state closes the color flow as illustrated by the dashed arrows in the top left hand diagram. This color flow implies that the eight diagrams in the third and fourth row vanish.

Compared to the contribution (3.1) from diagonal gluon exchanges, they are $O\left(1/(N_c^2-1)\right)$-suppressed.

The third and fourth row of figure 2 shows contributions with one diagonal and one off-diagonal gluon exchange. In contrast to a QED emission, these vanish in QCD since the color trace of one of the two source lines is $\propto \mathrm{Tr}\left[T^a\right]$ or $\propto \mathrm{Tr}\left[T^b\right]$.

The emission vertices (2.1) carry positive (negative) phases $\propto e^{i\mathbf{k}.\mathbf{y}_i}$ ($\propto e^{-i\mathbf{k}.\mathbf{y}_i}$) in the amplitude (complex conjugate amplitude). The squared amplitude can then be written easily,

$$\hat{\sigma}\left(\{\mathbf{k_1},\mathbf{k}_2\},\{\mathbf{y}_1,\mathbf{y}_2\}\right) \propto N_c^2\,\left(N_c^2-1\right)^2\left|\vec{f}(\mathbf{k}_1)\right|^2\,\left|\vec{f}(\mathbf{k}_2)\right|^2 \tag{3.3}$$

JHEP12(2017)074

$$\times\Bigg\{4+\frac{1}{(N_c^2-1)}\Big(e^{i(\mathbf{k}_1+\mathbf{k}_2).(\mathbf{y}_1-\mathbf{y}_2)}+e^{i(\mathbf{k}_1-\mathbf{k}_2).(\mathbf{y}_1-\mathbf{y}_2)} +e^{i(\mathbf{k}_1+\mathbf{k}_2).(\mathbf{y}_2-\mathbf{y}_1)}+e^{i(\mathbf{k}_1-\mathbf{k}_2).(\mathbf{y}_2-\mathbf{y}_1)}\Big)\Bigg\}.$$

Here, the leading factor 4 counts the four diagrams in the first row of figure 2, for which all gluon emissions are diagonal and thus all phases cancel. The four $O\left(1/(N_c^2-1)\right)$-suppressed phases in (3.3) correspond to the four diagrams in the second row of figure 2 (They are written in the same order in which they arise in the figure.) Here and in the following, we do not specify the normalization since it drops out of the correlation functions that we are interested in.

The two-gluon emission spectrum (2.2) can then be calculated for any given probability distribution $\rho\left(\{\mathbf{y}_i\}\right)$ of sources. In particular, for a Gaussian ansatz

$$\rho\left(\mathbf{y}_1,\mathbf{y}_2\right)=\frac{1}{(2\pi B)^2}\exp\left[-\frac{\mathbf{y}_1^2}{2B}-\frac{\mathbf{y}_2^2}{2B}\right], \tag{3.4}$$

that may be regarded as characterizing a collision at vanishing impact parameter for which the localization of sources does not have a statistically preferred azimuthal orientation, one finds after averaging over the relative distance $\Delta\mathbf{y}\equiv\mathbf{y}_1-\mathbf{y}_2$,

$$\frac{d\Sigma}{d\mathbf{k}_1 d\mathbf{k}_2}\propto\left|\vec{f}(\mathbf{k}_1)\right|^2\left|\vec{f}(\mathbf{k}_2)\right|^2\left[1+\frac{\left(e^{-B(\mathbf{k}_1+\mathbf{k}_2)^2}+e^{-B(\mathbf{k}_1-\mathbf{k}_2)^2}\right)}{(N_c^2-1)}\right]. \tag{3.5}$$

This is consistent with results obtained in [25–27]. The simple model defined in section 2.1 thus shares important commonalities with other approaches.[1]

Eq. (3.5) describes QCD dipole radiation. As the average distance $\langle\Delta\mathbf{y}\rangle\propto\sqrt{B}$ between the legs of the dipole increases, interference effects decrease and the second term in (3.5) becomes less important. It is a characteristic feature of the two-gluon emission spectrum (3.5) that interference effects enhance the emission equally for gluon pairs that are close in momentum space, $\mathbf{k}_1\approx\mathbf{k}_2$ and for those that are recoiling against each other, $\mathbf{k}_1\approx-\mathbf{k}_2$, [26]. Also, it has been noted repeatedly that spectra like (3.5) are symmetric with respect to $\mathbf{k}_i\to-\mathbf{k}_i$, so that they cannot give rise to odd harmonics [27]. The area B may be interpreted in terms of the inverse saturation scale $1/Q_s^2$ of a saturated parton density [25–27]. As we discuss in section 6, the ansatz (3.4) and a parameter range for B can also be motivated within the theory of multi-parton interactions.

We comment at this point on the physical interpretation of the two-gluon correlation in (3.5). This correlation arises from QCD interference of different production amplitudes but it should not be regarded as being the consequence of interference *between* the two gluons. Against the latter interpretation speaks the finding that an enhancement due to

[1] In eq. (37) of ref. [27] and in eq. (18) of ref. [25], the two-gluon spectrum was calculated from so-called glasma graphs. These calculations used a Gaussian average similar to (3.4), and they took a formal limit $2\pi Be^{-B(\mathbf{k})^2/2}\to(2\pi)^2\delta^{(2)}(\mathbf{k})$ while associating the factor $1/B$ with the inverse of a large but finite transverse surface. Expression (3.5) is consistent with these limiting cases and it matches the results given explicitly in ref. [26]. For a more thorough related derivation of the two-gluon spectrum, see also ref. [34].

JHEP12(2017)074

QCD interference is observed not only when the gluons sit close together in transverse momentum space (the term $e^{-B(\mathbf{k}_1-\mathbf{k}_2)^2}$ in (3.5)), but also when they are recoiling against each other (the term $e^{-B(\mathbf{k}_1+\mathbf{k}_2)^2}$ in (3.5)). Rather, the interference pattern in (3.5) is consistent with the picture that an azimuthal asymmetry in gluon emission arises for each gluon individually from the interference of the production amplitudes in which the gluon is linked to the first and the second source, respectively. What correlates the orientation of the two emitted gluons in azimuth is not their mutual interference but the fact that both are emitted from the *same* source pair. Since emission from a source dipole is symmetric with respect to the plane orthogonal to the dipole orientation, each gluon has the same propensity for ending up on the left or right hand side of that plane, and the probability of both gluons ending up in the same hemisphere (the term $e^{-B(\mathbf{k}_1-\mathbf{k}_2)^2}$ in (3.5)) or in opposite ones (the term $e^{-B(\mathbf{k}_1-\mathbf{k}_2)^2}$ in (3.5)) is therefore equal.

The above argument has noteworthy consequences beyond the simple example discussed in this subsection. First, for arbitrary gluon multiplicity m and arbitrary number of sources N, the diagrams with exactly 2 off-diagonal and $m-2$ diagonal gluons are of particular interest since they determine the full $O(1/(N_c^2-1))$ contribution to leading order in N (see next subsection). It follows from the color traces involved that these diagrams are only non-vanishing if both off-diagonal gluons connect to the same source pair. As a consequence, the above line of argument carries over to this more general case that we discuss in the next subsection. Second, the above discussion shows explicitly that gluons need not be close to each other in transverse momentum space to be correlated, since they are correlated via common sources. The analogous argument applies to the rapidity dependence. As long as the two sources used for the calculation (3.5) are eikonal and therefore emit gluons from the same transverse positions in different rapidity windows, the two gluons will be correlated in transverse momentum due to the dipole orientation of their common source pair and irrespective of their rapidity difference. This line of argument extends to all emission patterns studied in the present paper. We therefore expect that the omission of explicit rapidity dependencies in our model calculation does not change our conclusions qualitatively.

3.2 Dipole interference term for arbitrary $m > 2$ gluons from $N > 2$ sources

The calculation of the full interference pattern for emission of a large number m of gluons from a large number N of sources is difficult. Here, we consider first the simpler problem of calculating only the dipole interference terms that include $m-2$ diagonal and 2 off-diagonal gluons. This is the leading $O\left(1/(N_c^2-1)\right)$-correction to the emission spectrum

$$\begin{aligned}\hat{\sigma} \propto (N_c^2-1)^N N_c^m \left(\prod_{i=1}^{m}\left|\vec{f}(\mathbf{k}_i)\right|^2\right) \\ \times\Bigg\{N^m + F^{(2)}_{\mathrm{corr}}(N,m)\frac{N^{m-2}}{(N_c^2-1)}\sum_{(ab)}\sum_{(ij)} 4\cos\left(\mathbf{k}_a.\Delta\mathbf{y}_{ij}\right)\cos\left(\mathbf{k}_b.\Delta\mathbf{y}_{ij}\right) \\ +O\left(\frac{1}{N}\frac{1}{(N_c^2-1)}\right)+O\left(\frac{1}{(N_c^2-1)^2}\right)\Bigg\}. \end{aligned} \tag{3.6}$$

JHEP12(2017)074

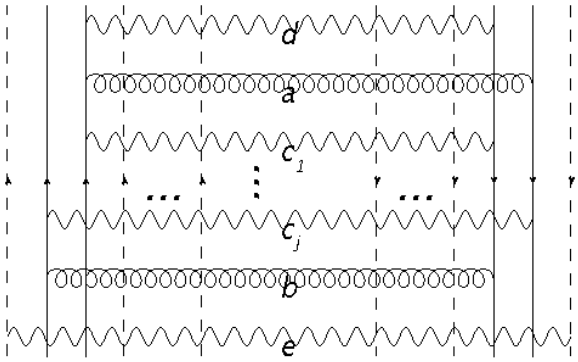

Figure 3. One specific contribution to the second term of the emission cross section (3.6) in which two off-diagonal gluons (curly lines) are supplemented by some diagonal gluons (zagged lines). The color trace associated to this particular contribution is $\mathrm{Tr}\left[T^e T^e\right] \mathrm{Tr}\left[T^{c_j} T^b T^{c_j} T^a\right] \mathrm{Tr}\left[T^{c_1} T^a T^d T^d T^{c_1} T^b\right] \mathrm{Tr}\left[\mathbb{1}\right]^2$. As argued in the text, each diagonal gluon that is sandwiched between the two off-diagonal ones and that links to the same sources as the off-diagonal ones (here, the gluons c_1 and c_j) results in a reduction of the color factor by 1/2. Therefore, diagonal gluons are not superimposed incoherently to the dipole interference pattern.

There are N^m possibilities of emitting incoherently m diagonal gluons from N sources. The color trace of an incoherent gluon emission gives one factor N_c for each of the m diagonal gluons and one factor (N_c^2-1) for each of the N sources. This explains the prefactor $(N_c^2-1)^N N_c^m\, N^m$ of the leading term in (3.6).

For the subleading term in (3.6), the factor N^{m-2} accounts for the number of choices of connecting $m-2$ diagonal gluons to N sources. The sum $\sum_{(ij)}$ goes over the $N(N-1)/2$ pairs of sources; the second term in (3.6) is therefore of the same order $O\left(N^m\right)$ as the first one. The dipole interference of two off-diagonal gluons suppresses this term by a factor $1/(N_c^2-1)$ compared to the leading one, as explained in section 3.1.

3.2.1 The color correction factor $F^{(2)}_{\mathrm{corr}}(N,m)$

To understand the factor $F^{(2)}_{\mathrm{corr}}(N,m)$ in (3.6), consider the color trace for a gluon emission diagram with one pair of off-diagonal gluons (colors a, b in figure 3) and with an arbitrary number of diagonal gluons. The following can be checked to be generally true: if a diagonal gluon is not connected to a source to which an off-diagonal gluon connects (color e in figure 3), or if it is connected to such a source but is not sandwiched between the two off-diagonal gluons (color d in figure 3), then the generators associated to this gluon emission stand always next to each other in some color trace and they simplify thus according to the color identity

$$T^d T^d = N_c\, \mathbb{1}\,. \tag{3.7}$$

In contrast, for those diagonal gluons that are sandwiched between the off-diagonal ones and that are connected to the same sources as the off-diagonal ones (colors c_1, c_j in figure 3), the generators in one of the color traces can always be brought into a form where they

JHEP12(2017)074

sandwich one of the generators of an off-diagonal gluon,

$$T^{c_j} T^a T^{c_j} = \frac{1}{2} N_c \, T^a \,. \tag{3.8}$$

For an ordered list of m gluons with one off-diagonal pair, there are $(m-1-j)$ possibilities of sandwiching $j = 0, \ldots, m-2$ diagonal gluons between the two off-diagonal ones. For each configuration with j sandwiched diagonal gluons, there are $\binom{j}{l} 2^l (N-2)^{j-l}$ possibilities of linking l of the sandwiched diagonal gluons to the sources to which the off-diagonal gluons are connected. Each such contribution is then suppressed by a correction factor $1/2^l$.

If one would ignore this correction factor $1/2^l$, one would assume that all $m-2$ diagonal gluons are incoherently superimposed to the interference pattern of the two off-diagonal gluons. The number of such incoherent superpositions is

$$\mathcal{N}_{\text{incoh}} = \sum_{j=0}^{m-2} N^{m-2-j} (m-1-j) \left(\sum_{l=0}^{j} \binom{j}{l} 2^l (N-2)^{j-l} \right) = \frac{m(m-1)}{2} \, N^{m-2} \,. \tag{3.9}$$

Taking into account that the sum $\sum_{(ab)}$ in (3.6) goes over $m(m-1)/2$ choices of selecting a pair of off-diagonal gluons from the ordered list, the factor $\mathcal{N}_{\text{incoh}}$ accounts for the N- and m-dependence of the prefactor of the $O\left(1/(N_c^2-1)\right)$-suppressed term in (3.6) if $F^{(2)}_{\text{corr}}(N,m)$ equals unity.

However, each of the l diagonal gluons that are sandwiched between the off-diagonal ones comes with an extra factor $1/2$ that corrects $\mathcal{N}_{\text{incoh}}$, and therefore

$$\begin{aligned} F^{(2)}_{\text{corr}}(N,m) &= \frac{1}{\mathcal{N}_{\text{incoh}}} \sum_{j=0}^{m-2} N^{m-2-j} (m-1-j) \left(\sum_{l=0}^{j} \binom{j}{l} 2^l (N-2)^{j-l} \frac{1}{2^l} \right) \\ &= \frac{2}{m(m-1)} N^{1-m} \left(N(N-1)^m + mN^m - N^{1+m} \right) . \end{aligned} \tag{3.10}$$

One finds $F^{(2)}_{\text{corr}}(N=2, m=2) = 1$, but in general, $F^{(2)}_{\text{corr}}(N,m) \leq 1$. For instance, $F^{(2)}_{\text{corr}}(3,3) = 8/9$ and $F^{(2)}_{\text{corr}}(4,4) = 27/32$ are consistent with cases explicitly calculated in the appendices A and B. We note the following limiting cases:

1. *The limit* $m = \text{const.}$, $N \to \infty$. Increasing the number of sources at fixed multiplicity m favors incoherent particle production and hence

$$\lim_{N\to\infty} F^{(2)}_{\text{corr}}(N,m)\Big|_{m=\text{const.}} = 1 \,. \tag{3.11}$$

   The same limiting value is reached for other color correction factors $F^{(*)}_{\text{corr}}(N,m)$ that we encounter in the next section.

2. *The limit* $m \to \infty$ *for fixed average multiplicity per source* $\overline{m} = m/N$. This limit is consistent with analyses of LHC pp data which indicate that the multiplicity of hard

processes is proportional to the soft multiplicity [41]. The color correction factors $F^{(*)}_{\rm corr}(N,m)$ are generally finite in this limit. In particular,

$$\lim_{m\to\infty} F^{(2)}_{\rm corr}(m/\overline{m},m) = \frac{2\overline{m}+2e^{-\overline{m}}-2}{\overline{m}^2}\,. \tag{3.12}$$

For $\overline{m}=1$, the correction factor (3.12) is $2/e\approx 0.73$, but for $\overline{m}=3$, it is 0.46 and for $\overline{m}=5$, it equals 0.32. So, higher event multiplicity per source leads to decorrelation that reduces the interference term in (3.6).

3. *The high-multiplicity limit $m\to\infty$ for fixed N.* For fixed number of sources, the color correction factor behaves asymptotically like

$$F^{(2)}_{\rm corr}(N,m)\Big|_{N=\text{const.}} \sim \frac{2\,N}{m} + O\left(\frac{N^2}{m^2}\right)\,. \tag{3.13}$$

Therefore, increasing multiplicity for a fixed number of sources leads to decorrelation.

3.2.2 The second order cumulant $v_2^2\{2\}$ to leading $O(1/N_c^2-1)$.

From the emission cross section (3.6) to order $O(1/N_c^2-1)$, one obtains from (2.7) the anisotropy coefficient

$$\begin{aligned} v_2^2\{2\}(k_1,k_2) &\equiv \langle\langle e^{i2(\phi_1-\phi_2)}\rangle\rangle(k_1,k_2) \\ &\equiv \frac{F^{(2)}_{\rm corr}(N,m)\int_\rho \frac{1}{N^2}\sum_{(ij)} 2^2 J_2\left(k_1\Delta y_{ij}\right)\,J_2\left(k_2\Delta y_{ij}\right)}{(N_c^2-1)+F^{(2)}_{\rm corr}(N,m)\int_\rho \frac{1}{N^2}\sum_{(ij)} 2^2 J_0\left(k_1\Delta y_{ij}\right)\,J_0\left(k_2\Delta y_{ij}\right)} \\ &= F^{(2)}_{\rm corr}(N,m)\frac{2^2}{(N_c^2-1)}\int_\rho \frac{1}{N^2}\sum_{(ij)} J_2\left(k_1\Delta y_{ij}\right)\,J_2\left(k_2\Delta y_{ij}\right) \\ &\quad + O\left(\frac{1}{(N_c^2-1)^2}\right)\,. \end{aligned} \tag{3.14}$$

Here, the Bessel functions J_2 arise from the ϕ-integration $\int_0^{2\pi} d\phi_a\, e^{i2\phi_a}\cos\mathbf{k}_a.(\mathbf{y}_i-\mathbf{y}_j)$ in (2.5) and we use $\Delta y_{ij}\equiv|\mathbf{y}_i-\mathbf{y}_j|$. The notational shorthand $\int_\rho$ stands for the averaging over source distributions as defined in (2.2), $\int_\rho\ldots\equiv\int\left(\prod_{i=1}^N d\mathbf{y}_i\right)\rho(\{y_i\})\ldots$. The sum $\sum_{(ab)}$ over the $m(m-1)/2$ possible pairs of off-diagonal gluon momenta drops out in calculating the average $\langle\langle e^{in(\phi_1-\phi_2)}\rangle\rangle$ in (2.7). We highlight three observations:

1. *For any multiplicity m, $v_2^2\{2\}$ is finite in the limit $N\to\infty$ of a large number of sources.* Since the sum $\sum_{(ij)}$ goes over $N(N-1)/2$ source pairs in (3.14), the two-particle cumulant $v_2^2\{2\}(k_1,k_2)$ approaches a finite value for $N\to\infty$. Physically, this is so since the observable $v_2^2\{2\}(k_1,k_2)$ sums over all source pairs, and since each source pair contributes with a $1/(N_c^2-1)$-suppressed contribution to two-particle interference terms. The signal strength $v_2^2\{2\}(k_1,k_2)$ does not decrease with the number of dipoles (or the multiplicity in the event) although each dipole is oriented in a statistically independent direction.

JHEP12(2017)074

2. $v_2^2\{2\}(k_1,k_2)$ *does not factorize except for small transverse momentum.* In general, due to the source average $\int_\rho$, one has $v_2^2\{2\}(k_1,k_2) \neq v_2\{2\}(k_1)\, v_2\{2\}(k_2)$. For a Gaussian source distribution (3.4), however, factorization holds for soft transverse momenta to leading order in Bk_1^2 and Bk_2^2,

$$v_2^2\{2\}(k_1,k_2) = F_{\rm corr}^{(2)}(N,m)\frac{1}{(N_c^2-1)}\left(Bk_1^2\right)\left(Bk_2^2\right) + O\left((Bk^2)^3\right) . \tag{3.15}$$

3. *For any finite number of sources* N, $v_2^2\{2\}(k_1,k_2)$ *vanishes in the high-multiplicity limit.* This is a direct consequence of (3.13). Based on intuition from QED, one may have expected that maximal azimuthal correlation arises if all gluons are emitted from the same color dipole (i.e., $N=2$). This is not the case. Emitting a large number m of gluons from a large number of sources N can yield a larger signal $v_2^2\{2\}(k_1,k_2)$ than emission from a small number of sources, since the color between off-diagonal gluons is less decorrelated.

4 Beyond 2nd order cumulants: results for leading $O(N)$ and up to subleading $O\left(1/(N_c^2-1)^3\right)$

We extend now the calculations of section 3 to the fourth order cumulant $v_2\{4\}$. To this end, we have calculated the m-gluon emission cross section from N sources up to $O\left(1/(N_c^2-1)^3\right)$. The result is[2] (see appendix B for details)

$$\begin{aligned}
\hat{\sigma} \propto\; & N_c^m\left(N_c^2-1\right)^N\left(\prod_{i=1}^m\left|\vec{f}(\mathbf{k}_i)\right|^2\right)N^{m-4} \\
&\times\Bigg\{N^4 + F_{\rm corr}^{(2)}(N,m)\frac{N^2}{(N_c^2-1)}\sum_{(ab)}\sum_{(lm)} 2^2\cos\left(\mathbf{k}_a.\Delta\mathbf{y}_{lm}\right)\cos\left(\mathbf{k}_b.\Delta\mathbf{y}_{lm}\right) \\
&\quad + F_{\rm corr}^{(3i)}(N,m)\frac{N}{(N_c^2-1)^2}\sum_{(abc)}\sum_{(lm)(mn)(nl)} 2^3\cos\left(\mathbf{k}_a.\Delta\mathbf{y}_{lm}\right) \\
&\qquad\qquad \times\cos\left(\mathbf{k}_b.\Delta\mathbf{y}_{mn}\right)\cos\left(\mathbf{k}_c.\Delta\mathbf{y}_{nl}\right) \\
&\quad + F_{\rm corr}^{(4i)}(N,m)\frac{1}{(N_c^2-1)^2}\sum_{(lm),(no)}\sum_{(ab)(cd)} 2^4\cos\left(\mathbf{k}_a.\Delta\mathbf{y}_{lm}\right)\cos\left(\mathbf{k}_b.\Delta\mathbf{y}_{lm}\right) \\
&\qquad\qquad \times\cos\left(\mathbf{k}_c.\Delta\mathbf{y}_{no}\right)\cos\left(\mathbf{k}_d.\Delta\mathbf{y}_{no}\right) \\
&\quad + F_{\rm corr}^{(4ii)}(N,m)\frac{1}{(N_c^2-1)^3}\sum_{(lm)(mn)(no)(ol)}\sum_{(abcd)} 2^4\cos\left(\mathbf{k}_a.\Delta\mathbf{y}_{lm}\right)\cos\left(\mathbf{k}_b.\Delta\mathbf{y}_{mn}\right) \\
&\qquad\qquad \times\cos\left(\mathbf{k}_c.\Delta\mathbf{y}_{no}\right)\cos\left(\mathbf{k}_d.\Delta\mathbf{y}_{ol}\right)
\end{aligned}$$

[2] In eq. (4.1) $\sum_{(abc)}$ sums over the $m(m-1)(m-2)/3!$ unordered triplets of outgoing momenta, i.e., each index a, b, c runs from 1 to m and the combinations (abc), (bac) and other permutations are counted like one element in the sum. Similarly, $\sum_{(lm)(mn)(nl)}$ sums over the $N(N-1)(N-2)$ unordered triplets of three source pairs made of three sources. In contrast, the comma in the sum $\sum_{(lm),(no)}$ indicates that this sum is over the $N(N-1)(N-2)(N-3)/2^2$ elements in the ordered set of doublets of source pairs, i.e., the entries $(lm),(no)$ and $(no),(lm)$ are counted separately.

JHEP12(2017)074

$$
\begin{aligned}
&+F^{(5)}_{\rm corr}(N,m)\frac{N^{-1}}{(N_c^2-1)^3}\sum_{[(lm)(mn)(nl)](op)}\sum_{(abc)(de)}2^2\cos\left(\mathbf{k}_d.\Delta\mathbf{y}_{op}\right)\cos\left(\mathbf{k}_e.\Delta\mathbf{y}_{op}\right)\\
&\qquad\times 2^3\cos\left(\mathbf{k}_a.\Delta\mathbf{y}_{lm}\right)\cos\left(\mathbf{k}_b.\Delta\mathbf{y}_{mn}\right)\cos\left(\mathbf{k}_c.\Delta\mathbf{y}_{nl}\right)\\
&+F^{(6)}_{\rm corr}(N,m)\frac{N^{-2}}{(N_c^2-1)^3}\sum_{(lm)(no)(pq)}\sum_{(ab)(cd)(ef)}2^2\cos\left(\mathbf{k}_a.\Delta\mathbf{y}_{lm}\right)\cos\left(\mathbf{k}_b.\Delta\mathbf{y}_{lm}\right)\\
&\qquad\times 2^2\cos\left(\mathbf{k}_c.\Delta\mathbf{y}_{no}\right)\cos\left(\mathbf{k}_d.\Delta\mathbf{y}_{no}\right)2^2\cos\left(\mathbf{k}_e.\Delta\mathbf{y}_{pq}\right)\cos\left(\mathbf{k}_f.\Delta\mathbf{y}_{pq}\right)\\
&+O\left(\frac{1}{N}\right)+O\left(\frac{1}{(N_c^2-1)^4}\right)\Bigg\}\,,
\end{aligned}
\tag{4.1}
$$

This expression contains color correction factors $F^{(*)}_{\rm corr}(N,m)$ that we determine in appendix C in close analogy to the derivation given in section 3.2.1 for $F^{(2)}_{\rm corr}(N,m)$.

In equation (4.1), only those contributions are written that are $O(N^m)$ and thus leading in the number of sources. To subleading order in the number of sources, there is a large number of additional interference diagrams. For instance, one can have four off-diagonal gluons emitted from one single source pair, and this contribution is $O(N^{-2})$ suppressed compared to the terms given in (4.1). For the cases $N=m=3$ and $N=m=4$, we have determined all these contributions explicitly in appendices A and B. These appendices provide combinatorical and calculational details on how to determine (4.1). However, we have neither calculated nor classified completely the subleading contributions $O(N^{-1})$ for an arbitrary number of sources N. For technical reasons, we therefore limit the present discussion to leading $O(N)$, which amounts to calculating $v_2\{4\}$ to $O(N^0)$.

We are particularly interested in the question to what extent interference effects could give rise to asymmetries in the final state momentum distributions even if there are no asymmetries in the initial source distributions. We therefore specialize to a factorized ansatz of the N-source distribution in terms of a product of azimuthally symmetric single-source probabilities,

$$
\rho\left(\{\mathbf{y}_j\}\right)=\prod_{j=1}^{N}\rho(\mathbf{y}_j)\,. \tag{4.2}
$$

This ansatz includes factorizing Gaussian source models at vanishing impact parameter $\mathbf{b}$, $\rho\left(\{\mathbf{y}_j\}\right)=\prod_{j=1}^{N}\left(\frac{1}{(2\pi B)}\exp(-\mathbf{y}_j^2/(2B))\right)$, that will be motivated further in section 6.

4.1 4-particle cumulant to $O(N^0)$ and $O\left(1/(N_c^2-1)^2\right)$

Restricting our discussion to the second harmonics, we define the normalized 4-point correlation function in terms of equations (2.9) and (4.1),

$$
\langle\langle e^{i2(\phi_1+\phi_2-\phi_3-\phi_4)}\rangle\rangle(k_1,k_2,k_3,k_4)=\frac{S_2(k_1,k_2,k_3,k_4)}{\overline{S}(k_1,k_2,k_3,k_4)}\,. \tag{4.3}
$$

Here, we discuss this expression first to leading order $O\left(1/(N_c^2-1)^2\right)$, when only one term of (4.1) contributes,

$$
\langle\langle e^{i2(\phi_1+\phi_2-\phi_3-\phi_4)}\rangle\rangle(k_1,k_2,k_3,k_4)=\frac{1}{(N_c^2-1)^2}\frac{2^4}{N^4}F^{(4i)}_{\rm corr}(N,k)
$$

JHEP12(2017)074

$$\times \int_\rho \sum_{(lm),(no)} \Big\{ J_2\left(k_1 \Delta y_{lm}\right)\, J_2\left(k_2 \Delta y_{lm}\right)\, J_2\left(k_3 \Delta y_{no}\right)\, J_2\left(k_4 \Delta y_{no}\right)\, e^{i4(\phi_{lm}-\phi_{no})}$$
$$+ J_2\left(k_1 \Delta y_{lm}\right)\, J_2\left(k_3 \Delta y_{lm}\right)\, J_2\left(k_2 \Delta y_{no}\right)\, J_2\left(k_4 \Delta y_{no}\right)$$
$$+ J_2\left(k_1 \Delta y_{lm}\right)\, J_2\left(k_4 \Delta y_{lm}\right)\, J_2\left(k_2 \Delta y_{no}\right)\, J_2\left(k_3 \Delta y_{no}\right) \Big\}$$
$$+ O\left(\frac{1}{N}\frac{1}{(N_c^2-1)^2}\right) + O\left(\frac{1}{(N_c^2-1)^3}\right) . \tag{4.4}$$

Here, the angles ϕ_{lm}, ϕ_{no} denote the azimuthal orientations of the dipoles (lm) and (no). For factorizing distributions of the type (4.2), different dipoles are not correlated in angular orientation, and the source average over the phase $e^{i4(\phi_{lm}-\phi_{no})}$ in the first term of (4.4) vanishes. With the help of the two-point function (3.12), the fourth order cumulant (2.10) can then be written in the following compact form

$$\langle\langle e^{i2(\phi_1+\phi_2-\phi_3-\phi_4)}\rangle\rangle_{\rm c}(k_1,k_2,k_3,k_4)$$
$$= \int_\rho \frac{F^{(4i)}_{\rm corr}(N,m)}{N^4} \Bigg\{ \left(\sum_{(lm),(no)} \frac{2^2}{(N_c^2-1)} J_2\left(k_1\Delta y_{lm}\right) J_2\left(k_3\Delta y_{lm}\right) \right)$$
$$\times \left(\frac{2^2}{(N_c^2-1)} J_2\left(k_2\Delta y_{no}\right)\, J_2\left(k_4\Delta y_{no}\right) \right) + (k_3 \longleftrightarrow k_4) \Bigg\}$$
$$- \int_\rho \left(\frac{F^{(2)}_{\rm corr}(N,m)}{N^2} \right)^2 \Bigg\{ \left(\sum_{(lm)} \frac{2^2}{(N_c^2-1)} J_2\left(k_1\Delta y_{lm}\right)\, J_2\left(k_3\Delta y_{lm}\right) \right)$$
$$\times \left(\frac{2^2}{(N_c^2-1)} \sum_{(no)} J_2\left(k_2\Delta y_{no}\right)\, J_2\left(k_4\Delta y_{no}\right) \right) + (k_3 \longleftrightarrow k_4) \Bigg\}$$
$$+ O\left(\frac{1}{N}\right) + O\left(\frac{1}{(N_c^2-1)^2}\right) . \tag{4.5}$$

For source distributions (4.2), all dipole configurations (lm), (no) make identical contributions. It is then sufficient to count the number of these dipoles. The sum $\sum_{(lm),(no)}$ in (4.5) goes over $N(N-1)(N-2)(N-3)/2^2$ doublets of source pairs and thus includes $N^4/4 + O(N^3)$ terms. Each of the sums $\sum_{(lm)}$ and $\sum_{(no)}$ in (4.5) go over $N(N-1)/2$ possibilities so that their product includes $N^4/4 + O(N^3)$ terms, too. To leading order in $1/N$, we can therefore replace in (4.5)

$$\left(\frac{F^{(4i)}_{\rm corr}(N,m)}{N^4} \left(\sum_{(lm),(no)} 1 \right) - \frac{F^{(2)}_{\rm corr}(N,m)}{N^2} \left(\sum_{(lm)} 1 \right) \frac{F^{(2)}_{\rm corr}(N,m)}{N^2} \left(\sum_{(no)} 1 \right) \right) \ldots$$
$$\longrightarrow \frac{1}{4} \left(F^{(4i)}_{\rm corr}(N,m) - \left(F^{(2)}_{\rm corr}(N,m) \right)^2 \right) + O\left(N^{-1}\right) . \tag{4.6}$$

To order $O\left(N^0\right)$, this expression vanishes. In more detail:

1. *In the limit* $m = \text{const.}$, $N \to \infty$, *all color correction factors in (4.1) become trivial,*

$$\lim_{N\to\infty} F^{(*)}_{\rm corr}(N,m)\Big|_{m=\text{const.}} = 1 . \tag{4.7}$$

JHEP12(2017)074

2. *In the limit $m \to \infty$, for fixed average multiplicity per source $\overline{m} = m/N$,*

$$\lim_{N\to\infty} F^{(2)}_{\rm corr}(N, N\overline{m})^2 = \lim_{N\to\infty} F^{(4i)}_{\rm corr}(N, N\overline{m}) = \left(\frac{2\overline{m} + 2e^{-\overline{m}} - 2}{\overline{m}^2}\right)^2 . \tag{4.8}$$

As a consequence, (4.6) vanishes in both limits and we find for the 4-particle cumulant to $O(N^0)$ and $O\left(1/(N_c^2-1)^2\right)$

$$v_2^4\{4\}(k_1,k_2,k_3,k_4) = 0 + O\left(1/N\right) + O\left(1/(N_c^2-1)^3\right) . \tag{4.9}$$

For the third limit discussed in section 3.2.1 ($m \to \infty$ for constant N), subleading terms in N would have to be kept. The present calculation therefore does not give access to this limit.

4.2 4-particle cumulant to $O(N^0)$ and $O\left(1/(N_c^2-1)^3\right)$

We extend now the calculation of the 4-particle cumulant (4.3) to order $O\left(1/(N_c^2-1)^3\right)$. All terms in (4.1) contribute to this order. In principle, the azimuthal integrations in (4.3) can be done analytically, and the result can be expressed in terms of source averages over Bessel functions. The resulting expression are straightforward to obtain but they are lengthy. They simplify significantly if one assumes Gaussian source distributions

$$\rho\left(\{\mathbf{y}_i\}\right) = \prod_{j=1}^{N}\left(\frac{1}{(2\pi B)}\exp\left[-\frac{\mathbf{y}_j^2}{2B}\right]\right) , \tag{4.10}$$

and if one limits the analysis to small transverse momenta $B\,k_i^2 \ll 1$. For part of the following discussion, we resort to this approximation in which the discussion of qualitative properties becomes more transparent.

To calculate $\langle\langle e^{i2(\phi_1+\phi_2-\phi_3-\phi_4)}\rangle\rangle_{\rm c}$ to $O\left(1/(N_c^2-1)^3\right)$ in (2.10), we need to calculate the two-point correlation function to $O\left(1/(N_c^2-1)^2\right)$, and for this we need to calculate the norm $\overline{T}(k_1,k_2)$ to $O\left(1/(N_c^2-1)^2\right)$. For the Gaussian source distribution (4.10) and to lowest order in transverse momenta, we find

$$\overline{T}(k_1,k_2) = \#\frac{m(m-1)}{2}N^4\left\{1 + \frac{2}{N_c^2-1}F^{(2)}_{\rm corr}\right\} + O\left(1/(N_c^2-1)^2\right) . \tag{4.11}$$

Here, the hash # denotes prefactors that are common to $\overline{T}$ and T and that will therefore drop out in the calculation of $\langle\langle e^{i2(\phi_1-\phi_2)}\rangle\rangle_{\rm c}$. (Essentially, the hash stands for the factors written in the first line of (4.1).) The numerator of (2.6) takes the form

$$\begin{aligned} T_2(k_1,k_2) = \#\frac{m(m-1)}{2}N^4\left(Bk_1^2\right)\left(Bk_2^2\right)\Bigg\{&\frac{F^{(2)}_{\rm corr}}{N_c^2-1} \\ &+ \frac{F^{(3)}_{\rm corr}}{(N_c^2-1)^2}(m-2) + \frac{F^{(4i)}_{\rm corr}}{(N_c^2-1)^2}(m-2)(m-3)\Bigg\} . \end{aligned} \tag{4.12}$$

JHEP12(2017)074

To leading order $O\left(1/(N_c^2-1)\right)$, the normalized azimuthal two-particle correlation function reduces then to (3.15), but there are higher order corrections

$$\begin{aligned}\langle\langle e^{i2(\phi_1-\phi_2)}\rangle\rangle(k_1,k_2) &\equiv \frac{T(k_1,k_2)}{\overline{T}(k_1,k_2)}\\ &= (Bk_1^2)\,(Bk_2^2)\left\{\frac{1}{(N_c^2-1)}\,F_{\rm corr}^{(2)}\right.\\ &\quad\left.+\frac{1}{(N_c^2-1)^2}\left(F_{\rm corr}^{(4i)}(m-2)(m-3)+F_{\rm corr}^{(3)}(m-2)-2(F_{\rm corr}^{(2)})^2\right)\right\}\\ &\quad+O\left(N^{-1}\right)+O\left(1/(N_c^2-1)^3\right)\,. \end{aligned}\tag{4.13}$$

The m-gluon emission cross section (4.1) includes contributions that involve interference between 3 or 4 off-diagonal gluons and that enter (4.12). For instance, the term proportional to $F_{\rm corr}^{(3)}$ in (4.12) includes a sum $\sum_{(abc)}$ over $m!/(3!(m-3)!)$ triplets of off-diagonal gluons. In the contribution of this term to $\langle\langle e^{i2(\phi_1-\phi_2)}\rangle\rangle(k_1,k_2)$, only those terms in $\sum_{(abc)}$ survive for which two of the three gluons match the phases. As a consequence, the sum reduces to $\sum_{(12c)}$, which is a sum over $(m-2)$ terms. This is the reason for the factor $F_{\rm corr}^{(3)}\,(m-2)$ in (4.13). The factor $(m-2)(m-3)$ multiplying $F_{\rm corr}^{(4i)}$ in (4.13) can be understood analogously. The factor $(F_{\rm corr}^{(2)})^2$ comes from expanding the normalization $1/\overline{T}$ to $O\left(1/(N_c^2-1)\right)$.

Analogously, one obtains the phase factor (2.9) which determines the numerator of the 4-particle correlation function $\langle\langle e^{i2(\phi_1+\phi_2-\phi_3-\phi_4)}\rangle\rangle$,

$$\begin{aligned}S_2(k_1,k_2,k_3,k_4) &= \#\begin{pmatrix}m\\4\end{pmatrix}\,N^4\,(Bk_1^2)\,(Bk_2^2)\,(Bk_3^2)\,(Bk_4^2)\\ &\quad\times\left\{\frac{1}{(N_c^2-1)^2}\,2\,F_{\rm corr}^{(4i)}\right.\\ &\quad\left.+\frac{1}{(N_c^2-1)^3}\left(2F_{\rm corr}^{(4ii)}+4F_{\rm corr}^{(5)}(m-4)+2F_{\rm corr}^{(6)}(m-5)(m-6)\right)\right\}\\ &\quad+O\left(N^{-1}\right)+O\left(1/(N_c^2-1)^4\right)\,. \end{aligned}\tag{4.14}$$

To write down $\langle\langle e^{i2(\phi_1+\phi_2-\phi_3-\phi_4)}\rangle\rangle$ to $O\left(1/(N_c^2-1)^3\right)$, one needs the normalization $\overline{S}$ to $O\left(1/(N_c^2-1)\right)$ since (4.14) starts at $O\left(1/(N_c^2-1)^2\right)$. One finds, in close analogy to (4.11),

$$\overline{S}(k_1,k_2,k_3,k_4) = \#\begin{pmatrix}m\\4\end{pmatrix}\,N^4\left\{1+\frac{2}{N_c^2-1}F_{\rm corr}^{(2)}\right\}+O\left(1/(N_c^2-1)^2\right)\,.\tag{4.15}$$

These expressions define $\langle\langle e^{i2(\phi_1+\phi_2-\phi_3-\phi_4)}\rangle\rangle$ according to (4.3). The resulting connected 4-particle correlation function (2.10) reads

$$\begin{aligned}\langle\langle e^{i2(\phi_1+\phi_2-\phi_3-\phi_4)}\rangle\rangle_c &= (Bk_1^2)(Bk_2^2)(Bk_3^2)(Bk_4^2)\\ &\quad\times\left\{\frac{1}{(N_c^2-1)^2}\left(2F_{\rm corr}^{(4i)}-2F_{\rm corr}^{(2)}F_{\rm corr}^{(2)}+O\left(N^{-1}\right)\right)\right.\\ &\quad\left.+\frac{1}{(N_c^2-1)^3}\left(2F_{\rm corr}^{(6)}(m-4)(m-5)-4F_{\rm corr}^{(2)}F_{\rm corr}^{(4i)}(m-2)(m-3)\right.\right.\end{aligned}$$

JHEP12(2017)074

$$+4F_{\rm corr}^{(5)}(m-4)-4F_{\rm corr}^{(2)}F_{\rm corr}^{(3)}(m-2)$$
$$+2F_{\rm corr}^{(4ii)}+8\left(F_{\rm corr}^{(2)}\right)^3-4F_{\rm corr}^{(4i)}F_{\rm corr}^{(2)}\Big)+O\left(N^{-1}\right)\Big\}$$
$$+O\left(1/(N_c^2-1)^4\right). \tag{4.16}$$

We discuss now limiting cases of this expression.

4.2.1 The limit $N \to \infty$ for constant multiplicity m to order $O(1/(N_c^2-1)^3)$

Following eq. (4.7), all color correction factors reduce to unity in this limit, and the connected 4-point correlation function (4.16) reads

$$\langle\langle e^{i2(\phi_1+\phi_2-\phi_3-\phi_4)}\rangle\rangle_c = (Bk_1^2)\,(Bk_2^2)\,(Bk_3^2)\,(Bk_4^2)\,\frac{2}{(N_c^2-1)^3}\left(7+m-m^2\right)$$
$$+O\left(1/(N_c^2-1)^4\right). \tag{4.17}$$

According to equation (2.11), the 4-th order cumulant defines a real-valued 4-th order anisotropy coefficient $v_2\{4\}$ only if it is negative. Remarkably, this condition is satisfied for sufficiently large multiplicity m, since (4.17) turns negative for $m > 3.7$. The m^2-term in (4.17) will dominate for relatively small multiplicities already (say for $m > 5$), and the 4-th order cumulant reads then

$$v_2\{4\}(k) \simeq \frac{1}{(N_c^2-1)^{3/4}} 2^{1/4}\sqrt{m}\,B\,k^2\,. \tag{4.18}$$

We conclude that without any azimuthal asymmetry in the initial state [see eq. (4.10)] and without any (coupling-constant dependent) interaction in the final state, QCD interference can give rise to non-vanishing negative fourth-order cumulants that have an interpretation in terms of azimuthal harmonics $v_2\{4\}(k)$. In this sense, our calculation provides a proof of principle that the baseline of vanishing interaction in the final state and of vanishing azimuthal correlation in the initial state does not correspond to a vanishing value $v_2\{4\}(k)$.

Equation (4.18) provides a proof of principle for the arguments above, but its range of validity is limited as we discuss now. We have calculated $v_2\{2\}(k)$ and $v_2\{4\}(k)$ to leading order in the number of sources and in the large-N_c limit. In particular, the second order cumulant (4.13) contains a leading term $\propto F_{\rm corr}^{(2)}/(N_c^2-1)$ and a subleading term $\propto F_{\rm corr}^{(4i)}m^2/(N_c^2-1)^2$. A similar observation can be made for the 4-particle correlator (4.16) where the term suppressed by one power $1/(N_c^2-1)$ is enhanced by m^2. This seems to indicate that the expansion in powers of $1/(N_c^2-1)$ converges only as long as $m^2 < (N_c^2-1)$.

The radius of convergence may be larger than the above estimate for the following reason: in equations (4.13) and (4.16), terms proportional to m (m^2) arise from integrating out the transverse momentum q of one (two) of the off-diagonal gluons involved in an interference term. In the simplest case,[3] this q-integration leads to contributions of the type

$$a \equiv \frac{\int d\mathbf{q}\int d\mathbf{z}\,J_0(qz)\,\rho(\mathbf{z})\,f(\mathbf{q})^2}{\int d\mathbf{q}\,|\vec{f}(\mathbf{q})|^2}\,. \tag{4.19}$$

[3]For instance, the contribution to (4.12) obtained from integrating the term proportional to $F_{\rm corr}^{(3i)}$ in (4.1) over the third transverse momentum $\mathbf{k}_c$ yields $(m-2)$ choices of the transverse momentum $\mathbf{k}_c$. Accordingly, the contribution to the two-particle correlator (4.13) is $\propto F_{\rm corr}^{(3i)}\,a\,(m-2)$.

JHEP12(2017)074

For technical simplicity, we have worked in this subsection to lowest order in small transverse momentum. This amounts to the assumption that the emission vertex $f(\mathbf{q})$ is dominated by transverse momenta that are much smaller than the inverse transverse size of the source. In this limit, $J_0(qz) \approx 1$ and thus $a = 1$. In general, however, $a \leq 1$. Indeed, depending on the emission vertices $f(\mathbf{q})$ and on the source density $\rho(\mathbf{z})$, a may be significantly smaller than unity, and e.g. the $F_{\rm corr}^{(3i)}$-term in (4.13) should yield a contribution $\propto F_{\rm corr}^{(3i)}\,(m-2)\,a$.

Integrating out transverse gluon momenta from other contributions in (4.1) can yield more complicated expressions than (4.19), but the maximal value is always obtained in the limit $B\,q^2 \ll 1$ studied here, and the value starts decreasing when the integral over the transverse momentum extends to values that start resolving the transverse distance between sources. Therefore, rather than being limited to $m^2 < (N_c^2-1)$, the region of validity of the calculations in section 4 is expected to extend up to higher multiplicities

$$m_{\rm max} \sim \sqrt{N_c^2-1}/a\,, \tag{4.20}$$

where $a \ll 1$. Physically, a is a penalty factor for integrating out off-diagonal gluons. It depends on the source size and the emission vertex f.

4.2.2 $N \to \infty$ for constant average multiplicity $\overline{m}$ to order $O(1/(N_c^2-1)^3)$

In the limit $N \to \infty$ for fixed average multiplicity $\overline{m} \equiv m/N$, the color correction factors satisfy several interesting identities. Defining $F_{\rm corr}^{(*)}(\overline{m}) \equiv \lim_{N\to\infty} F_{\rm corr}^{(*)}(N, N\overline{m})$, one finds

$$F_{\rm corr}^{(4i)}(\overline{m}) = F_{\rm corr}^{(2)}(\overline{m})\,F_{\rm corr}^{(2)}(\overline{m})\,, \tag{4.21}$$
$$F_{\rm corr}^{(5)}(\overline{m}) = F_{\rm corr}^{(3)}(\overline{m})\,F_{\rm corr}^{(2)}(\overline{m})\,, \tag{4.22}$$
$$F_{\rm corr}^{(6)}(\overline{m}) = F_{\rm corr}^{(2)}(\overline{m})\,F_{\rm corr}^{(2)}(\overline{m})\,F_{\rm corr}^{(2)}(\overline{m})\,. \tag{4.23}$$

One may use these relations to simplify the connected 4-particle correlation function (4.16),

$$\begin{aligned}\langle\langle e^{i2(\phi_1+\phi_2-\phi_3-\phi_4)}\rangle\rangle_c = {}& \frac{1}{(N_c^2-1)^3}(Bk_1^2)(Bk_2^2)(Bk_3^2)(Bk_4^2)\\ &\times\Big\{\Big(F_{\rm corr}^{(2)}\Big)^3(-2m^2+2m+20)-8F_{\rm corr}^{(2)}F_{\rm corr}^{(3)}+2F_{\rm corr}^{(4ii)}+O\big(N^{-1}\big)\Big\}\\ &+O\big(1/(N_c^2-1)^4\big)\,.\end{aligned} \tag{4.24}$$

As in the limit of section 4.2.1, this expression is negative for sufficiently large multiplicity $m \gtrsim 4$ and thus lends itself to a collective interpretation of $v_2\{4\}$. However, since the limit $N \to \infty$ at constant $\overline{m}$ implies $m \to \infty$, one cannot parallel the argument of section 4.2.1 that the expansion is well-defined for sufficiently small multiplicity m. To take this limit, one would need information about subleading orders in N. [For instance, if there were terms of $O(N^{-1})$ in (4.24) that are enhanced by $\sim m^3$, then these would contribute to leading order in the limit $N \to \infty$ at constant $\overline{m}$.]

JHEP12(2017)074

4.3 6-particle cumulant to $O(N^0)$ and $O\left(1/(N_c^2-1)^3\right)$

From equation (4.1), we can also evaluate the expectation value $\langle\langle e^{i2(\phi_1+\phi_2+\phi_3-\phi_4-\phi_5-\phi_6)}\rangle\rangle$ to order $O\left(1/(N_c^2-1)^3\right)$. Since the numerator of this expression starts at $O\left(1/(N_c^2-1)^3\right)$, the normalization is trivial. One finds from explicit calculation in the limit $(Bk_i^2) \ll 1$

$$\begin{aligned}
&\langle\langle e^{i2(\phi_1+\phi_2+\phi_3-\phi_4-\phi_5-\phi_6)}\rangle\rangle(k_1,k_2,k_3,k_4,k_5,k_6) \\
&\quad = (Bk_1^2)\,(Bk_2^2)\,(Bk_3^2)\,(Bk_4^2)\,(Bk_5^2)\,(Bk_6^2)\frac{1}{(N_c^2-1)^3}\,6\,F_{\rm corr}^{(6)} \\
&\qquad + O\left(1/(N_c^2-1)^4\right)\,. \qquad (4.25)
\end{aligned}$$

The 6-th particle cumulant is defined as $\langle\langle 6\rangle\rangle_c \equiv \langle\langle 6\rangle\rangle - 9\langle\langle 2\rangle\rangle\langle\langle 4\rangle\rangle + 12\langle\langle 2\rangle\rangle^3$ (in this shorthand notation, the numbers in brackets denote the number of phases). One therefore finds

$$\begin{aligned}
&\langle\langle e^{i2(\phi_1+\phi_2+\phi_3-\phi_4-\phi_5-\phi_6)}\rangle\rangle_c(k_1,k_2,k_3,k_4,k_5,k_6) \\
&\quad = (Bk_1^2)\,(Bk_2^2)\,(Bk_3^2)\,(Bk_4^2)\,(Bk_5^2)\,(Bk_6^2)\frac{1}{(N_c^2-1)^3} \\
&\qquad \times\left\{6\,F_{\rm corr}^{(6)} - 18\,F_{\rm corr}^{(2)}\,F_{\rm corr}^{(4i)} + 12\,\left(F_{\rm corr}^{(2)}\right)^3\right\} + O\left(1/(N_c^2-1)^4\right) \\
&\quad = 0 + O\left(1/(N_c^2-1)^4\right)\,. \qquad (4.26)
\end{aligned}$$

Here, the fact that the contribution of $O\left(1/(N_c^2-1)^3\right)$ vanishes to leading $O(1/N)$ is a consequence of

$$\lim_{N\to\infty}\left\{6\,F_{\rm corr}^{(6)} - 18\,F_{\rm corr}^{(2)}\,F_{\rm corr}^{(4i)} + 12\,\left(F_{\rm corr}^{(2)}\right)^3\right\} = 0\,. \qquad (4.27)$$

This limit vanishes, irrespective of whether it is taken for fixed multiplicity m or for fixed average multiplicity $\overline{m} = m/N$. The latter statement is checked easily with the help of eqs. (4.21)–(4.23). Consistent with our finding (4.9) that the term proportional to $1/\sqrt{N_c^2-1}$ vanishes in $v_2\{4\}$, we find therefore that $v_2\{6\}$ vanishes to the same order.

We did not check whether (4.26) vanishes to order $O\left(1/(N_c^2-1)^4\right)$. If it would not vanish (and if it would have a positive sign), then $v_2\{6\} \sim O(1/(N_c^2-1)^{2/3})$. This would be peculiar, as $v_2\{6\}$ would then be parametrically larger than $v_2\{4\}$. It is also conceivable that the first non-vanishing order to $v_2\{6\}$ is $O\left(1/(N_c^2-1)^5\right)$. In this case, $v_2\{6\} \sim O(1/(N_c^2-1)^{5/6})$ would be parametrically smaller than $v_2\{4\}$. In this case, the second, fourth and sixth cumulant would follow the systematics $v_2\{2k\} \sim O\left(1/(N_c^2-1)^{(2k-1)/2k}\right)$ which would support the idea that higher order cumulants take similar values. These are open questions that lie outside the scope of the present manuscript. They would involve significant further calculations, but we believe that they can be addressed with the techniques used in this section.

5 Higher harmonics

In sections 3 and 4, we have focussed on the calculation of the second harmonics $\langle\langle e^{i2(\phi_1-\phi_2)}\rangle\rangle$ and $\langle\langle e^{i2(\phi_1+\phi_2-\phi_3-\phi_4)}\rangle\rangle_c$. Here, we discuss the calculation of other even and odd harmonics.

JHEP12(2017)074

5.1 Higher even harmonics

When calculating $\langle\langle e^{in(\phi_1-\phi_2)}\rangle\rangle$ and $\langle\langle e^{in(\phi_1+\phi_2-\phi_3-\phi_4)}\rangle\rangle_c$, one encounters elementary azimuthal integrals of the form

$$\int d\phi\, e^{in\phi} \cos\left(q\Delta y \cos(\phi)\right) . \tag{5.1}$$

Here, q is the modulus of a generic transverse momentum, Δy is the modulus of a generic transverse dipole separation, and ϕ is the relativ azimuthal angle between transverse momentum and dipole separation. All cosine-terms in (4.1) can be written as $\cos\left(q\Delta y \cos(\phi)\right)$ for suitable choices of q, Δy, and ϕ.

The integrals (5.1) are non-vanishing for all even integers n. For $n = 2$, one finds for instance

$$\begin{aligned}\int d\phi\, e^{i2\phi} \cos\left(q\Delta y \cos(\phi)\right) &= -2\pi J_2\left(q\Delta y\right) \\ &= \frac{-\pi}{4}\left(q\Delta y\right)^2 + O\left((q\Delta y)^4\right) .\end{aligned} \tag{5.2}$$

This leads to the Bessel functions J_2 in the calculation of the two-particle correlation (3.14) and the four particle correlation (4.4). Explicit expressions can also be given for higher even harmonics. For instance

$$\begin{aligned}\int d\phi\, e^{i4\phi} \cos\left(q\Delta y \cos(\phi)\right) &= 2\pi\, J_4\left(q\Delta y\right) \\ &= \frac{\pi}{192}\left(q\Delta y\right)^4 + O\left((q\Delta y)^6\right) .\end{aligned} \tag{5.3}$$

With the help of these expressions, the analysis of section 4 could be repeated for arbitrary even harmonics. Since the small-q limit of (5.1) is $\propto q^n$, one concludes immediately that the small-k-behavior of $v_n(\mathbf{k})$ is $\propto k^n$. In particular, the parametric dependence of the fourth harmonic at small q is $\sim (q\Delta y)^4$ while that of the second harmonics is $\sim (q\Delta y)^2$. Within the approximation of small transverse momenta, $\sim (B\, q^2) \ll 1$ explored in section 4.2, this implies that $v_4 \propto v_2\, v_2$ for second and fourth order cumulants. We discuss this point further in section 7.

5.2 Higher odd harmonics

In contrast to the even harmonics, the integral (5.1) vanishes for odd integers n. As a consequence, the odd harmonic flow coefficients v_n vanish up to $O\left(1/(N_c^2-1)^4\right)$ and $O\left(1/N\right)$, since the spectrum (4.1) shows only cosine-terms to this order.

Based on the idea that interference patterns are momentum conjugates of spatial distributions, one may naively expect that odd harmonics make some (possibly subleading) non-vanishing contribution whenever the spatial distribution shows odd harmonic eccentricities, i.e., for $N \geq 3$ sources. Motivated by this idea, we have calculated in appendix A all terms contributing to $N = m = 3$ in search of odd harmonics. However, the emission spectrum for $N = m = 3$ turned out to be free of odd harmonics.

JHEP12(2017)074

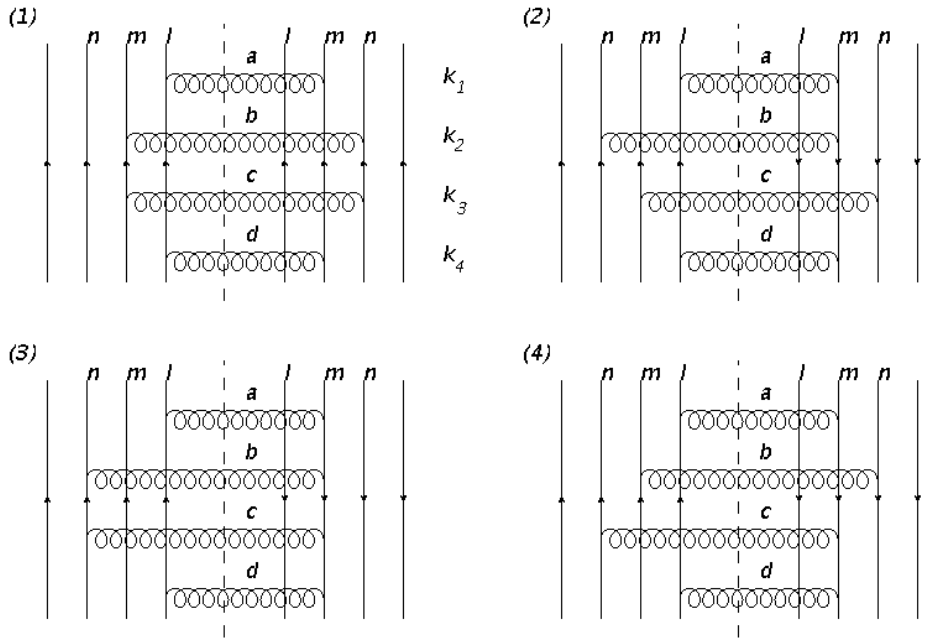

Figure 4. A set of diagrams that contribute to the sin-terms in (B.13), and thus to odd azimuthal harmonics.

5.2.1 Odd harmonics for the case $N = m = 4$

We have classified and calculated in appendix B all contributions to the emission spectrum for $N = m = 4$. Two classes of diagrams were found to lead to odd harmonics, see eqs. (B.13) and (B.15). Referring for technical details and explicit results to the appendix, we limit the discussion here in the main text to provide qualitative insight into how properties of the SU(N_c) color algebra can give rise to odd harmonics. To this end, we consider in figure 4 a set of diagrams with four off-diagonal gluons that are emitted from three sources l, m, n that combine to two pairs of sources (lm), (mn) .

For this contribution, one checks easily that the color trace changes depending on whether the sandwiched gluons of momentum $\mathbf{k}_2$ and $\mathbf{k}_3$ link from m to n or from n to m. For the four diagrams in figure 4, one finds

$$\begin{aligned}
&\mathrm{Tr}\,[\mathbb{1}]\ \mathrm{Tr}\left[T^c\,T^b\right]\ \mathrm{Tr}\left[T^b\,T^c\,T^d\,T^a\right]\ \mathrm{Tr}\left[T^a T^d\right] = N_c^4\,\left(N_c^2-1\right)^2 && \text{[for figure 4(1)]}\\
&\mathrm{Tr}\,[\mathbb{1}]\ \mathrm{Tr}\left[T^b\,T^c\right]\ \mathrm{Tr}\left[T^c\,T^d\,T^b\,T^a\right]\ \mathrm{Tr}\left[T^a\,T^d\right] = \frac{1}{2}N_c^4\,\left(N_c^2-1\right)^2 && \text{[for figure 4(2)]}\\
&\mathrm{Tr}\,[\mathbb{1}]\ \mathrm{Tr}\left[T^b\,T^c\right]\ \mathrm{Tr}\left[T^d\,T^c\,T^b\,T^a\right]\ \mathrm{Tr}\left[T^a\,T^d\right] = N_c^4\,\left(N_c^2-1\right)^2 && \text{[for figure 4(3)]}\\
&\mathrm{Tr}\,[\mathbb{1}]\ \mathrm{Tr}\left[T^c\,T^b\right]\ \mathrm{Tr}\left[T^b\,T^d\,T^c\,T^a\right]\ \mathrm{Tr}\left[T^a\,T^d\right] = \frac{1}{2}N_c^4\,\left(N_c^2-1\right)^2 && \text{[for figure 4(4)]}
\end{aligned}$$

Combining the factors 1/2 of these color traces with the $\mathbf{k}_2$- and $\mathbf{k}_3$-dependent phase factors of the four diagrams in figure 4, we find

$$\begin{aligned}
&e^{i\,\mathbf{k}_2.\boldsymbol{\Delta}\mathbf{y}_{mn}}\left(e^{i\,\mathbf{k}_3.\boldsymbol{\Delta}\mathbf{y}_{mn}}+\frac{1}{2}e^{-i\,\mathbf{k}_3.\boldsymbol{\Delta}\mathbf{y}_{mn}}\right)+e^{-i\,\mathbf{k}_2.\boldsymbol{\Delta}\mathbf{y}_{mn}}\left(\frac{1}{2}e^{i\,\mathbf{k}_3.\boldsymbol{\Delta}\mathbf{y}_{mn}}+e^{-i\,\mathbf{k}_3.\boldsymbol{\Delta}\mathbf{y}_{mn}}\right)\\
&\quad=3\cos\left(\mathbf{k}_2.\boldsymbol{\Delta}\mathbf{y}_{mn}\right)\,\cos\left(\mathbf{k}_3.\boldsymbol{\Delta}\mathbf{y}_{mn}\right)-\sin\left(\mathbf{k}_2.\boldsymbol{\Delta}\mathbf{y}_{mn}\right)\,\sin\left(\mathbf{k}_3.\boldsymbol{\Delta}\mathbf{y}_{mn}\right)\,. \qquad (5.4)
\end{aligned}$$

JHEP12(2017)074

For each diagram that contributes with a phase $e^{-i\,\mathbf{k}_j\cdot\mathbf{\Delta y}_{mn}}$, there is a diagram in which the off-diagonal gluon with momentum $\mathbf{k}_j$ links from m to n rather than from n to m while all other gluons are linked in the same way. If the prefactors of both these diagrams were the same, then these phases would add to a term $e^{-i\,\mathbf{k}_j\cdot\mathbf{\Delta y}_{mn}} + e^{+i\,\mathbf{k}_j\cdot\mathbf{\Delta y}_{mn}}$ that is proportional to a cosine, and odd harmonics in $\mathbf{k}_j$ would not occur. In the example above, it is only the non-abelianess of SU(N_c) that leads to different prefactors of the phases $e^{-i\,\mathbf{k}_j\cdot\mathbf{\Delta y}_{mn}}$ and $e^{+i\,\mathbf{k}_j\cdot\mathbf{\Delta y}_{mn}}$, thus giving rise to terms that change sign under $\mathbf{k}_j \to -\mathbf{k}_j$, see eq. (5.4). This is true for all odd harmonics that we have found in our calculations.

5.2.2 General comments on odd harmonics

In calculations of multi-particle correlations in the framework of saturation physics [28, 30–32, 34–36], it has been a persistent problem to find non-vanishing values of odd harmonic anisotropy coefficients such as v_3. Solutions to this problem include the proposal that the proton wavefunction consists of a few patches in the transverse plane in each of which color fields point in preferred direction [33], as well as the recent observation that odd harmonics arise as a high parton density effect directly from the non-linear QCD evolution [29]. The calculation in section 5.2.1 points to a third possible origin of odd harmonic contributions: without any coupling-constant dependent interaction in the initial or final state and without any asymmetry in the initial state, odd harmonic contributions to multi-particle production can arise from non-abelian properties of QCD interference.

For the odd harmonic contributions analyzed in section 5.2.1, it was important that the number of off-diagonal gluons was larger than the number of sources to which they were connected. As a consequence, these contributions seem to be $O(1/N)$-suppressed. We note, however, that we have studied odd harmonic contributions only for $N = m = 4$. We did not try to determine the color correction factor when further diagonal gluons are added to the diagrams studied here (this would require combinatorical arguments that go beyond those developped in appendix C), and we do not know the full N- and m-dependence of the leading odd harmonic contribution. It remains an interesting open question to find a classification of all diagrams of $O(1/N)$ and to establish how odd harmonics manifest themselves in the limit of a large number of sources.

6 Relation to the theory of multi-parton interactions (MPIs)

Starting from ideas in the mid-80s [42, 43], the treatment of multiple parton interactions (MPIs) in perturbative QCD has been developed further in recent years [44–53]. Here, we give simple arguments that relate this theory to the model defined in section 2 and that motivate values for the source parameter B in pp collisions.

Hadronic cross sections involving N partonic interactions are customarily parametrized as products of N independent parton-parton interactions σ_i

$$\sigma_{N\,\mathrm{MPI}} = \frac{\sigma_1 \ldots . \sigma_N}{K_N}\,. \tag{6.1}$$

The physics of MPIs enters here in the coefficient K_N that parametrizes deviations from an incoherent superposition of N interactions. K_N is dimensionfull $\propto (\mathrm{area})^{N-1}$. For the

JHEP12(2017)074

case of double parton interactions ($N = 2$), K reduces to the effective cross section $\sigma_{\rm eff}$ that is constrained experimentally. Under certain mild assumptions (such as neglecting contributions to MPIs from $1 \to 2$ splittings), K_N can be expressed through N-particle Generalized Parton Distributions (GPDs) G_N [46]

$$\frac{1}{K_N} = \int \left(\prod_{i=1}^{N} \frac{d\mathbf{\Delta}_i}{(2\pi)^2} \right) \frac{G_N(\{x_i\}, \{Q_i^2\}, \{\mathbf{\Delta}_i\})\, G_N(\{x_i'\}, \{Q_i^2\}, \{\mathbf{\Delta}_i\})}{\prod_{i=1}^{N} (f(x_i, Q_i^2)\, f(x_i', Q_i^2))} \delta^{(2)} \left(\sum_{i=1}^{N} \mathbf{\Delta}_i \right) . \tag{6.2}$$

Here $f(x, Q^2)$ denotes the standard single parton distribution function. The x_i, $\mathbf{\Delta}_i$ denote the longitudinal momentum fractions and the initial transverse momenta of the i-th parton in the incoming hadronic wave function. Neglecting the weak dependence of this expression on x_i and Q_i, K_N can be expressed in terms of the function

$$F_N(\mathbf{\Delta}_1, \ldots \mathbf{\Delta}_N) = \frac{G_N^2(\mathbf{\Delta}_1, \ldots \mathbf{\Delta}_N)}{\prod_{i=1}^{N} f(x_i, Q_i)\, f(x_i', Q_i)} . \tag{6.3}$$

For a process involving N MPIs, an m-parton production cross section can then be written formally as

$$\frac{d\sigma_N(\{\mathbf{k}_i\}, \{\mathbf{\Delta}_i\})}{d\mathbf{k}_1 \ldots d\mathbf{k}_m} \sim |\mathcal{M}^2(\{\mathbf{k}_i\}; \{\mathbf{\Delta}_i\})|\, F_N^2\,(\mathbf{\Delta}_1, \ldots, \mathbf{\Delta}_N)\; \delta^{(2)} \left(\sum_{j=1}^{N} \mathbf{\Delta}_j \right) \sigma_1 \ldots \sigma_N\,, \tag{6.4}$$

where $\mathcal{M}^2$ is the squared amplitude for the production of m gluons from N partons in the nucleon wave function ("N sources"). The corresponding m-particle spectrum is obtained by normalizing this expression with the cross section

$$\sigma_N = \prod \int d\mathbf{\Delta}_i\, F_N^2\,(\mathbf{\Delta}_1, \ldots, \mathbf{\Delta}_N)\; \delta^{(2)} \left(\sum_{j=1}^{N} \mathbf{\Delta}_j \right) \sigma_1 \ldots \sigma_N\,. \tag{6.5}$$

To arrive at eqs. (6.4) and (6.5), one assumes that m-parton production can be formulated in a pQCD factorized formalism. Here, we do not try to quantify corrections to this assumption. Rather, we treat a bold extrapolation of this perturbative approach to soft momenta as one way of getting insight into soft multi-particle production.

To see the commonalities between the model in section 2 and this formalism deduced from MPI theory, we introduce one further approximation by writing the generalized N-parton distribution functions G_N in a mean-field approximation [46] as products of generalized one-particle distribution functions $G_1(x, Q, \Delta) = f(x, Q)\, F_{2g}(\Delta)$ [54–56] with a two-gluon form factor that parametrizes the transverse momentum distribution

$$G_N(\{x_i\}, \{Q_i^2\}, \{\mathbf{\Delta}_i\}) = \prod_{i=1}^{N} G_1(x_i, Q_i, \mathbf{\Delta}_i) = \prod_{i=1}^{N} f(x_i, Q_i) F_{2g}(\mathbf{\Delta}_i)\,. \tag{6.6}$$

Choosing $F_{2g}^2(\Delta) = \exp(-B\Delta_i^2)$ for simplicity to be of Gaussian form (other functional dependencies could be explored), one has $F_N(\Delta_1, \ldots, \Delta_N) = \prod_{i=1}^{N} \exp(-B\Delta_i^2)$, and it is

JHEP12(2017)074

straightforward to switch from (6.5) to coordinate space representation[4]

$$\frac{d\sigma_N}{\sigma_N\, d\mathbf{k}_1 \dots d\mathbf{k}_m} = \frac{\int \left(\prod_{i=1}^N d\mathbf{y}_i\right) \int d\mathbf{b}\, |\mathcal{M}^2(\mathbf{k}_1, \cdots, \mathbf{k}_m; \mathbf{y}_1, \cdots, \mathbf{y}_N)| \rho(\mathbf{y}_1 \dots \mathbf{y}_N, \mathbf{b})}{\int \left(\prod_{i=1}^N d\mathbf{y}_i\right)\, d\mathbf{b}\, \rho(\mathbf{y}_1 \dots \mathbf{y}_N, \mathbf{b})}. \quad (6.7)$$

This is the form of the m-particle emission spectrum (2.2) with a source probability distribution ρ of the form (4.2). In section 2, we have supplemented the structure of (6.7) with a particularly simple model for calculating $\hat{\sigma} = |\mathcal{M}^2|$. Here, we see that this structure arises from MPI theory once one treats N-parton GPDs in mean field approximation.

We note that this framework allows one to constrain the parameter B in the source density by data. Namely, $1/K_N = \int d\mathbf{b} \prod d\mathbf{y}_i\, \rho(\{\mathbf{y}_i\}, \mathbf{b}) = 1/N(4\pi B)^{N-1}$, and therefore $\sigma_{\text{eff}} = K_2 = 8\pi B$,

$$B = 2\,\text{GeV}^{-2} \qquad \longleftrightarrow \qquad \sigma_{\text{eff}} \approx 20\,\text{mb} \quad (6.8)$$

Experimentally favored values for σ_{eff} lie in the range of 15 ± 5 mb for pp collisions at the LHC [57–59] and for $p\bar{p}$ collisions at Tevatron [60]. Somewhat higher values σ_{eff} of order 35–40 mb have been obtained in a mean field approach that does not include other mechanisms for MPI enhancement [48, 61]. This will prompt us in the next section to scan values in the range $1\,\text{GeV}^{-2} < B < 4\,\text{GeV}^{-2}$.

7 Numerical results

Whenever there are multiple partons in the final state, QCD interference contributes to the azimuthal anisotropies v_n for both even (see sections 3 and 4) and odd (see section 5) harmonics. This raises the question how contributions from QCD interference compare in size and signature to those of other physically conceivable mechanisms. What is the typical signal size with which QCD interference can contribute to v_n? And what is the expected p_T-, rapidity- and multiplicity-dependence of the effects discussed here? The present study is not sufficient to provide complete answers to these questions, but we summarize in this section what can be said from parametric considerations and from first numerical results.

Parametrically, leading contributions to v_n, n even, are $O\left(1/(N_c^2-1)^{1/2}\right)$ for the second order cumulants and $O\left(1/(N_c^2-1)^{3/4}\right)$ for the fourth-order cumulants. This N_c-dependence is multiplied by functions that grow $\propto |\mathbf{k}|^n$ for very small transverse momenta but that reach magnitudes of $O(1)$ for sufficiently large transverse momenta, see, e.g., eq. (3.14). For $N_c = 3$, signal sizes $v_n \sim 0.1 - 0.3$ seem therefore conceivable. The signal size is roughly independent of the number of sources N. While our analysis of the multiplicity dependence of v_n in section 4 does not allow us to draw conclusions in

[4]Here, the density $\rho\,(\{\mathbf{y}_i\}, \mathbf{b})$ is a convolution of the normalized densities of colliding partons in the two incoming hadrons. For a Gaussian ansatz

$$\rho\,(\{\mathbf{y}_i\}, \mathbf{b}) = \prod_j \frac{1}{(4\pi B)^2} \exp\left[-\frac{\mathbf{y}_j^2}{4B}\right] \exp\left[-\frac{(\mathbf{y}_j - \mathbf{b})^2}{4B}\right].$$

In other sections, we have used this distribution for vanishing impact parameter $\mathbf{b} = 0$ and normalized to unity, see eq. (4.2).

JHEP12(2017)074

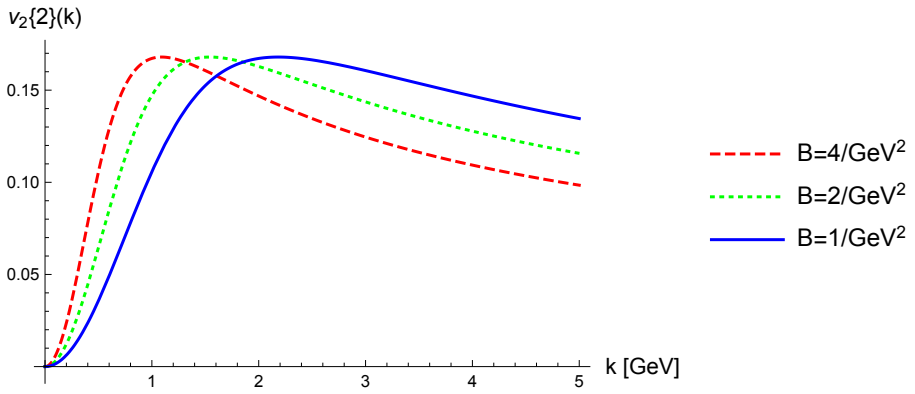

Figure 5. The 2nd order cumulant $v_2\{2\}(k) = \sqrt{v_2^2\{2\}(k,k)}$ evaluated from (3.14) for $F^{(2)}_{\rm corr} = 1$.

the limit of large multiplicity, it points to the possibility that v_n rises with multiplicity. Also, the model described in section 2 leads naturally to an approximately flat rapidity dependence. Albeit not established on the quantitative level needed for decisive tests, the above-mentioned features agree at least qualitatively with trends in the data.

It is less clear whether also the transverse momentum dependence of the interference effects studied here can account for the qualitative trends in the data. Amplitudes for the emission from different sources are expected to interfer only for sufficiently small transverse momenta k that do not resolve the separation Δy between the emitters, $k < 1/\Delta y$. It is therefore unclear whether QCD interference can contribute significantly to $v_n(k)$ in the multiple GeV range where significant signal strength is observed. To address this question, we plot in figure 5 the transverse momentum dependence of the second order cumulant for values of the source parameter B favored by data on multi-parton interactions, see eq. (6.8). The main qualitative features of this second order cumulant are indeed consistent with main trends in the data, the signal strength increases up to transverse momenta of 2 GeV and a sizeable signal persists in the multi-GeV range.

As seen from figure 6, the signal size obtained in the present formalism varies linearly with the value of the color correction factor. The color correction factors used in figure 6 are for an average of $\bar{m} = 3$ or 5 emitted particles per source, but a more extreme choice $\bar{m} = 20$ that may be at the upper end of what is phenomenologically viable would reduce the signal by $F^{(2)}_{\rm corr} = 0.1$. In comparison to these uncertainties, the $O(1/(N_c^2 - 1))$- corrections in the denominator of (3.14) turn out to be negligible.

We next point to the fact that $v_2^2\{2\}(k_1, k_2)$ does not factorize. To this end, we show in the upper panel of figure 7 the ratio $v_2^2\{2\}(k_1, k_2)/v_2\{2\}(k_1)\, v_2\{2\}(k_2)$. One sees that in the transverse momentum range up to ~ 1.5 GeV, deviations from factorization are at most $\sim 20\%$. For higher transverse momenta, however, particle emission starts to decorrelate as soon as the difference between the transverse momenta of the two emittees is larger than 1–2 GeV. For the experimentally measured hadronic momentum correlations, such

JHEP12(2017)074

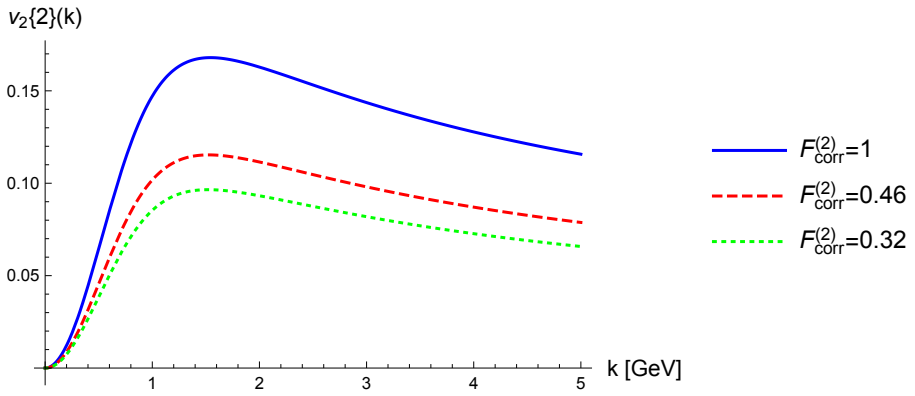

Figure 6. The 2nd order cumulant as in figure 5 for $B = 2/\text{GeV}^2$ but now compared to values of the color correction factor $F^{(2)}_{\text{corr}} = 0.45$ (0.32) that correspond to an average of $\overline{m} = 3$ (5) emitted particles per source.

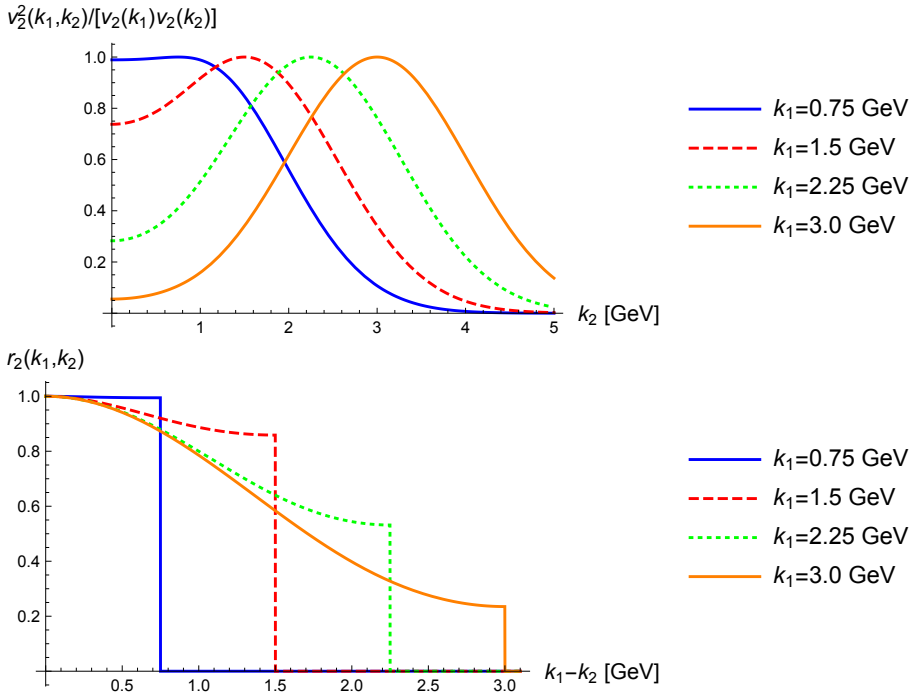

Figure 7. Upper panel: illustration of factorization breaking $v_2^2\{2\}(k_1, k_2) \neq v_2\{2\}(k_1)\, v_2\{2\}(k_2)$. Lower panel: the corresponding factorization ratio $r_2(k_1, k_2)$ as defined in equation (7.1), plotted for selected 'trigger' momenta k_1 against the relative momentum difference $k_1 - k_2$.

JHEP12(2017)074

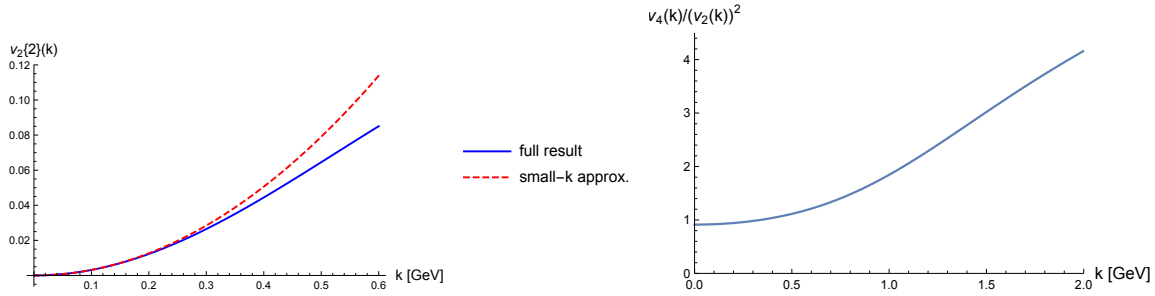

Figure 8. L.h.s.: comparison of the second cumulant $v_2\{2\}(k)$ calculated from (3.14), and the approximation (4.13) for small transverse momentum. R.h.s.: the ratio of $v_4\{2\}(k)$ and $(v_2\{2\}(k))^2$ that is known to be constant in the limit of small transverse momentum. Both calculations are for $B = 2/GeV^2$ and $F^{(2)}_{\rm corr} = 1$.

deviations from factorization are often characterized in terms of the factorization ratio

$$r_2(k_1, k_2) = \frac{v_2\{2\}(k_1, k_2)}{\sqrt{v_2\{2\}(k_1)\, v_2\{2\}(k_2)}}\,, \tag{7.1}$$

where one of the two momenta, say k_1, is regarded as trigger, and the other is the associate particle satisfying $k_2 < k_1$. The corresponding quantity is plotted in the lower panel of figure 7 as a function of $k_1 - k_2$. For pPb and PbPb collisions, the factorization ratio $r_2(k_1, k_2)$ has been measured at LHC [62] and it is in agreement with fluid dynamic simulations [63], see also ref. [64] for earlier discussions of the relation of $r_2(k_1, k_2)$ to fluid dynamics. Figure 7 shows features qualitatively similar to those reported in refs. [62, 63] in that r_2 decreases with increasing $k_1 - k_2$ and that this decrease is more pronounced for increasing trigger k_1. Clearly, the present calculation is for pp collisions, and it shows a correlation on parton level. Hadronization may be expected to affect the correlation r_2 significantly as it tends to smear and soften transverse momentum distributions. Given these substantial differences between the results of refs. [62, 63] and the present calculation, we refrain from a quantitative comparison.

In section 4, we have limited one part of our discussion to the small-k approximation in which many expressions simplify. The left hand side of figure 8 indicates the range of validity of this approximation. As discussed in section 5.1, it is a structural property of the small-k approximation that

$$v_4\{2\}(k) = \text{const.}\; v_2\{2\}(k)\, v_2\{2\}(k)\,. \tag{7.2}$$

Similar relations between different harmonic coefficients are known to arise in fluid dynamic models as a consequence of mode-mode coupling [65–67]. For the specific relation (7.2), it was noted already in ref. [68] that one expects for large transverse momentum a proportionality constant 1/2. It is therefore interesting to note that non-trivial relations between v_4 and v_2 may also arise from mechanisms that do not invoke interactions in the final state. The right hand side of figure 8 illustrates this point further. For small k, v_4 is seen to be approximately proportional to $(v_2)^2$ with a proportionality factor of order unity.

JHEP12(2017)074

So far, the figures shown in this section were calculated to leading order in $1/(N_c^2-1)$ from the second order cumulant (3.14). To the next order in $1/(N_c^2-1)$, the second order cumulant $v_2\{2\}(k)$ receives an additive correction, see eq. (4.13). However, as explained in section 4, this is an expansion in powers of $m^2/(N_c^2-1)$ that does not converge for large multiplicities. An analogous statement applies to the 4-th order cumulant $v_2\{4\}(k)$ in equation (4.16) for which the contribution subleading in $1/(N_c^2-1)$ grows with m^2. Despite this caveat, we proceed here with a numerical exploration of $v_2\{4\}(k)$. To this end, we focus on the term $\propto m^2$ in (4.16) that dominates for large multiplicity. Rather than going to the small-k-limit (4.18), we keep the color correction factor in (4.16), and we re-establish the large-k-behavior by replacing Bk^2 with the integral over Bessel functions from which it was obtained in a small-k-approximation,

$$v_2^4\{4\}(k) \approx \frac{\left(F_{\rm corr}^{(2)}(N,m)\right)^3}{(N_c^2-1)^3} 2\,d\,m^2 \left(\int_\rho J_2\left(k_1\Delta y\right)\, J_2\left(k_2\Delta y\right)\right)^2 . \tag{7.3}$$

Here, d denotes a suppression factor that arises from integrating out one of the three dipoles in the term $\propto F_{\rm corr}^{(6)} = \left(F_{\rm corr}^{(2)}\right)^3$ in (4.1). The factor d equals unity for $B\,k^2 \ll 1$ but it depends on the vertex function and can be smaller than unity $d<1$. For any given vertex function $f(k)$, it can be calculated in close analogy to the suppression factor a in (4.19) and one has $d \sim O(a^2)$.

Figure 9 shows the fourth root of (7.3) for multiplicities m reached in high-multiplicity proton-proton collisions at the LHC, and for a number of sources N comparable to the number of MPIs invoked in MC simulations of the underlying event of such pp collisions. We also vary the suppression factor d over ranges that are easily obtained from (4.19) and $d \simeq a^2$. While the results in figure 9 fall short of a quantitative determination of $v_2^4\{4\}(k)$, they support the qualitative statement that the size and shape of the 4-th order cumulant $v_2\{4\}(k)$ resulting from QCD interference may be comparable to the size and shape of the second order cumulants $v_2\{2\}(k)$ within the parameter range realized in high-multiplicity proton-proton collisions.

8 Conclusion

Whenever multiple partons are produced in a hadronic collision, there are interference effects whose size varies with the momentum distribution and the colors of the outgoing partons. These QCD interference effects do not depend on α_s. In this sense, they are part of a "no-interaction" baseline for v_n that needs to be controlled prior to discussing non-linear dynamics in the incoming hadronic wavefunctions or rescattering and fluid dynamization in the final state.[5]

[5]This α_s-independence distinguishes the QCD interference effects discussed here from other conceivable interference effects. For instance, in ref. [69], an initial state multiple scattering bremsstrahlung picture with recoil effects was explored as a source for finite harmonic flow coefficients in pA-collisions. This is based on an LPM interference effect that is clearly unrelated to the interference effects studied in the present paper. The effects discussed in ref. [69] are therefore expected to die out in the dilute limit when secondary scattering becomes unimportant while the effects included in our no-interaction baseline persist.

JHEP12(2017)074

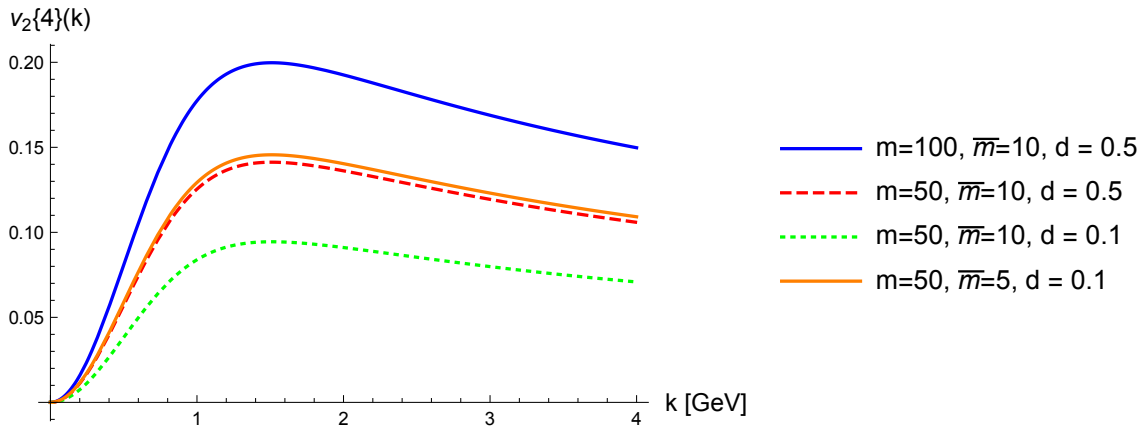

Figure 9. Approximation (7.3) of the 4-th order cumulant $v_2^4\{4\}(k)$ for different multiplicities m, average multiplicities $\overline{m}$ per source and values of the suppression factor d, obtained from intergrating out one dipole radiation factor.

Here we have used a simple model of multi-particle production (see section 2) to estimate how these QCD interference effects can contribute to the azimuthal anisotropy coefficients v_n measured with second and higher order cumulants in pp collisions. We have pointed out (section 6) that this model can be realized in the mean field theory of multi-parton interactions (MPIs), with MPIs representing the "sources" of individual parton-parton collisions and radiated gluons corresponding to radiation associated with the MPIs.

Our calculations establish that the contribution of QCD interference to the anisotropy coefficients v_n, n even, persists unattenuated for an increasing number of sources, that it can increase with increasing multiplicity, and that it persists in higher order cumulants. We have further shown that odd harmonic anisotropy coefficients arise due to the non-abelianness of the QCD interference pattern.[6] In section 7, we have supplemented these structural results about how the QCD interference impacts anisotropy coefficients with a first numerical exploration. Both, the order of magnitude of the calculated v_n, as well as the shape of their transverse momentum dependence was found to be of the order of magnitude and shape of the signals observed in pp collisions at the LHC. Given the simple nature of the model in section 2 (schematic treatment of particle production, absence of hadronization, etc.), these qualitative commonalities between model and data must not be over-interpreted. However, they make it certainly conceivable that the no-interaction baseline including QCD interference effects can make a sizeable if not dominant contribution to the measured v_n coefficients in pp collisions.

This leads naturally to the question whether and to what extent QCD interference effects could contribute also to the anisotropy coefficients measured in AA collisions. Here, however, marked differences need to be considered. First, jet quenching provides unambiguous experimental evidence for significant final state rescattering which is an α_s-dependent

[6] The mechanism via which odd harmonics arise is parametrically different: the contributions are $O(1/N)$, but they can be enhanced by powers of m and work is needed to estimate them in the phenomenologically relevant parameter range.

JHEP12(2017)074

microscopic mechanism that underlies hydrodynamization and that can translate spatial gradients into momentum anisotropies. Given the strength of jet quenching signals, it is thus inconceivable that QCD interference can account for the totality of the observed v_n signals in AA. Second, final state scattering can destroy coherence and the resulting interference. While QCD interference clearly shifts the no-interaction baseline for v_n, it is therefore questionable that effects of interactions contribute additively on top of this baseline. Rather than seeking a common explanation of v_n across system size, it may therefore also be instructive to explore the opposite hypothesis, namely that the physics mechanisms underlying the v_n-signals in pp and AA are qualitatively different, being dominated by QCD interference for pp while being dominated by fluid dynamics for AA. The similarities in the experimental signal of pp, pA and AA may be viewed as disfavouring this hypothesis, but the qualitatively different evidence for final state rescattering in both systems suggests that different mechanisms are at work in pp and AA and these may therefore also be at the origin of the measured v_n. The present work adds to this discussion only by illustrating that QCD interference may account for the order of magnitude and main qualitative features of v_n signals in pp. As far as pA collisions are concerned, the absence of experimental evidence for significant final state scattering supports the idea that the qualitative conclusions about QCD interference drawn here for pp carry over to pA.

We have aimed at controlling in this paper interference effects between an arbitrary number m of gluons emitted from an arbitrary number N of sources. This was achieved within an expansion in powers of $1/(N_c^2-1)$ and to leading order in N by resumming the effects of an arbitrary number of diagonal gluons in color correction factors. We hope that these results can be useful also for the discussion of other models, such as models based on saturation physics[7] that encompass QCD interference effects and with which our calculation agrees to lowest order, see eq. (3.5). Within these models, the importance of QCD interference effects has been emphasized repeatedly (see e.g. ref. [39]), but they are not studied in isolation and are difficult to disentangle from effects of finite partonic density. Indeed, due to the greater complexity of calculations in these models, correlation functions have not been analyzed to the same level of detail as in the present manuscript, and we are not aware of similar parametric statements about the leading N-independence and $1/(N_c^2-1)$-dependence of higher order cumulants.

Future developments may also better relate the results reported here to recent efforts of improving MC simulations of the underlying event in TeV-scale proton-proton collisions. On the one hand, while all modern multi-purpose MC event generators model the underlying event in terms of multi-parton interactions, the QCD interference effects discussed here are not included in these simulations. On the other hand, there are efforts to go beyond an essentially incoherent superposition of MPIs supplemented with conservation laws, e.g. by modeling effects of overlapping strings and studying whether these could give rise to sig-

[7] In the notation of section 2, the initial transverse density of sources is $\sim N/B$. Since the $v_2\{2\}$ and $v_2\{4\}$ calculated in section 4 are N-independent and finite to leading order in $1/N$, a high or saturated initial parton density is not a prerequisite for the effects discussed here while it is the basis of calculations in the so-called CGC-formalism.

JHEP12(2017)074

natures of collectivity [70–72]. For earlier works, see e.g. ref. [73] and approaches based on pomeron dynamics [74, 75]. It would be interesting to understand how QCD interference can be included in MC simulations and how this compares e.g. to effects of overlapping strings or other models.

Finally, within the set-up of this manuscript, the expansion in $O\left(1/(N_c^2-1)\right)$ analyzed here provided first qualitative insights, but we also discussed its limitations. In particular, a more systematic control over $1/N$-suppressed terms may allow for more quantitative statements in the range of multiplicity and number of sources that are phenomenologically interesting, and it would give access to odd harmonic anisotropy coefficients. Moreover, to gain better control in the phenomenologically interesting range of multiplicities, one would ideally like to resum all contributions that come with powers in $m^2/(N_c^2-1)$. We expect that such further advances are possible.

Acknowledgments

B.B., C.J. and M.S. thank the CERN TH Department for hospitality and support during short stays in 2016 and 2017. C.J. was supported by the Conselho Nacional de Desenvolvimento Cientifico e Tecnológico (CNPq). M.S.'s research was supported by the US Department of Energy Office of Science, Office of Nuclear Physics under Award No. DE-FG02-93ER40771.

A Multi-gluon emission for $N = m = 3$

In this appendix, we calculate the cross section for producing $m = 3$ gluons from $N = 3$ sources. This will illustrate several statements that we have generalized to arbitrary N and m in the main text.

For N sources and m emitted gluons, there are N^{2m} different diagrams, since each of the m gluons can be attached to any of the N sources in the amplitude, and to any of the N sources in the complex conjugate amplitude. For $N = m = 3$, these $N^{2m} = 3^6$ diagrammatic contributions can be classified as follows:

I 3 diagonal gluons (27 diagrams)

II 2 diagonal gluons and 1 off-diagonal gluon (6×27 diagrams)

III 1 diagonal gluon and 2 off-diagonal gluons (12×27 diagrams)

IV 3 off-diagonal gluons (8×27 diagrams)

To illustrate how to enumerate these diagrams, consider, e.g., case II: there are 3 choices for the source to which each of the diagonal gluon can be attached. For the off-diagonal gluon, one has 3 choices for the source in the amplitude times 2 choices in the complex conjugate amplitude. As exactly one of the three gluons is off-diagonal, one has also 3 choices for selecting the off-diagonal gluon amongst all three gluons. Combining these factors leads to $3 \times 3 \times (3 \times 2) \times 3 = 6 \times 27$ different diagrams.

JHEP12(2017)074

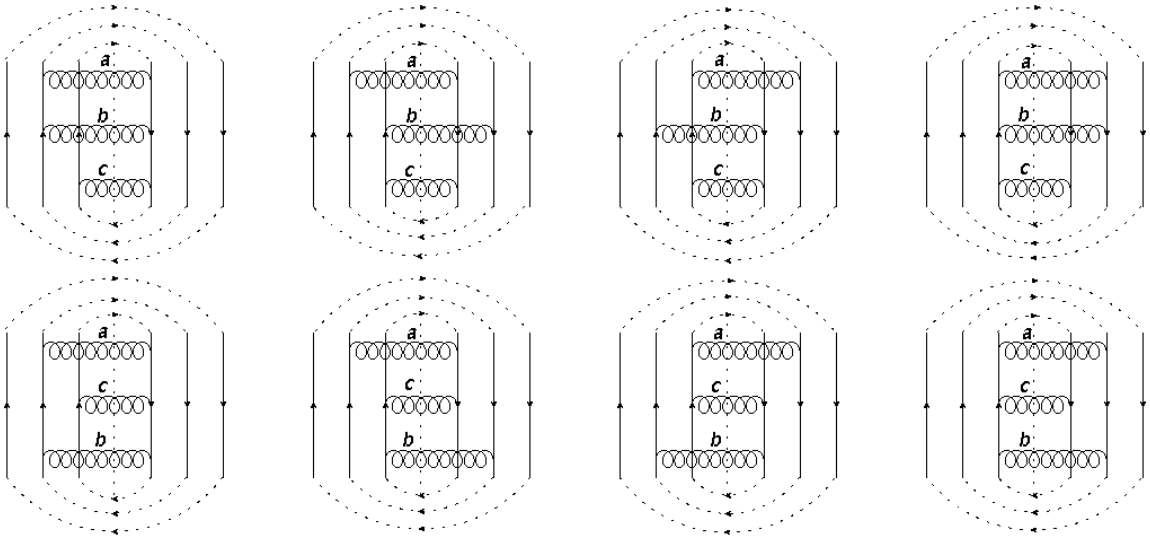

Figure 10. Some of the contributions with two off-diagonal and one diagonal gluon that contribute to the $k = 3$-gluon radiation spectrum from $N = 3$ sources. The color factor (A.2) for diagrams in the top row is twice as large as the color factor (A.3) for those in the bottom row.

We turn now to the calculation of the different contributing cases: for three diagonal gluons radiated off three sources (**case I**), all 27 diagrams contributing to the 3-gluon radiation cross section have the same color factor $(N_c^2-1)^3 N_c^3$. As phase factors cancel for diagonal gluons, the contribution to $\hat{\sigma}$ is

$$\hat{\sigma}_I\left(\{\mathbf{k_1},\mathbf{k}_2,\mathbf{k}_3\},\{\mathbf{y}_1,\mathbf{y}_2,\mathbf{y}_3\}\right) \propto (N_c^2-1)^3 N_c^3 \left|\vec{f}(\mathbf{k}_1)\right|^2 \left|\vec{f}(\mathbf{k}_2)\right|^2 \left|\vec{f}(\mathbf{k}_3)\right|^2 27\,. \tag{A.1}$$

One also checks easily that the color factors of all diagrams with only 1 off-diagonal gluon (**case II**) vanish,

$$\hat{\sigma}_{II} = 0\,. \tag{A.2}$$

Case III includes 8×27 diagrams for which the two off-diagonal gluons connect to three sources; these have vanishing color factors. In addition, there are 4×27 diagrams for which the two off-diagonal gluons connect to two sources. For those, we denote with a and b the colors of the off-diagonal gluons and with c the color of the diagonal one. If the diagonal gluon links to the source that is not touched by the off-diagonal gluons (case not shown in figure 10), then the resulting color factor is $\mathrm{Tr}\left[T^cT^c\right]\mathrm{Tr}\left[T^aT^b\right]\mathrm{Tr}\left[T^aT^b\right] = N_c^3(N_c^2-1)^2$. If the diagonal gluon touches instead a source that is also touched by the off-diagonal gluons, but is not sandwiched between the off-diagonal gluons (see, e.g., top row of figure 10), then

$$\mathrm{Tr}\left[1\right]\mathrm{Tr}\left[T^cT^cT^aT^b\right]\mathrm{Tr}\left[T^aT^b\right] = N_c^3(N_c^2-1)^2\,. \tag{A.3}$$

However, for those diagrams for which the diagonal gluon is sandwiched between the off-diagonal ones and for which the diagonal and off-diagonal ones have one source in common (see second row of figure 10), one finds

$$\mathrm{Tr}\left[1\right]\mathrm{Tr}\left[T^cT^aT^cT^b\right]\mathrm{Tr}\left[T^aT^b\right] = \frac{1}{2}N_c^3(N_c^2-1)^2\,. \tag{A.4}$$

JHEP12(2017)074

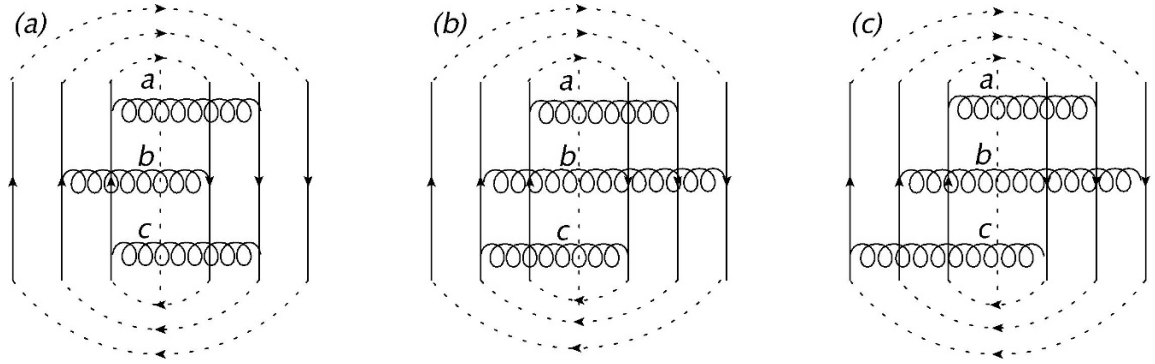

Figure 11. Examples for diagrammatic contributions with 3 off-diagonal gluons that link between one (a), two (b) and three (c) different pairs of sources. Contributions of type (b) vanish while contributions of type (a) and (c) have color traces that differ by a factor $(N_c^2-1)/4$, see text for more details.

The total contribution of the diagrams of case III to the 3-gluon emission cross section takes then the form

$$\begin{aligned}\hat{\sigma}_{III}^{(ord)}\left(\{\mathbf{k_1},\mathbf{k}_2,\mathbf{k}_3\},\{\mathbf{y}_1,\mathbf{y}_2,\mathbf{y}_3\}\right) \propto (N_c^2-1)^3 N_c^3 \left|\vec{f}(\mathbf{k}_1)\right|^2 \left|\vec{f}(\mathbf{k}_2)\right|^2 \left|\vec{f}(\mathbf{k}_3)\right|^2 \\ \times\Bigg\{ \frac{3}{(N_c^2-1)}\sum_{(ij)} 4\cos\left(\mathbf{k}_1.\Delta\mathbf{y}_{ij}\right)\cos\left(\mathbf{k}_2.\Delta\mathbf{y}_{ij}\right) \\ +\frac{2}{(N_c^2-1)}\sum_{(ij)} 4\cos\left(\mathbf{k}_1.\Delta\mathbf{y}_{ij}\right)\cos\left(\mathbf{k}_3.\Delta\mathbf{y}_{ij}\right) \\ +\frac{3}{(N_c^2-1)}\sum_{(ij)} 4\cos\left(\mathbf{k}_2.\Delta\mathbf{y}_{ij}\right)\cos\left(\mathbf{k}_3.\Delta\mathbf{y}_{ij}\right)\Bigg\}. \end{aligned} \tag{A.5}$$

Here, we use the subscript *(ord)* to indicate that the momenta $\mathbf{k}_1$, $\mathbf{k}_2$ and $\mathbf{k}_3$ are ordered from top to bottom in the emission diagrams. The color trace (A.4) appears only for 2 of the 3 diagrams for which the diagonal gluon carries $\mathbf{k}_2$, and this reduces the prefactor of the second term in (A.5) to $2\times 1/2+1=2$.

Following (2.3), we randomize the external momenta to obtain

$$\begin{aligned}\hat{\sigma}_{III}\left(\{\mathbf{k_1},\mathbf{k}_2,\mathbf{k}_3\},\{\mathbf{y}_1,\mathbf{y}_2,\mathbf{y}_3\}\right) \propto (N_c^2-1)^3 N_c^3 \left|\vec{f}(\mathbf{k}_1)\right|^2 \left|\vec{f}(\mathbf{k}_2)\right|^2 \left|\vec{f}(\mathbf{k}_3)\right|^2 \\ \times\frac{8}{3(N_c^2-1)}\frac{N}{3}\sum_{(ab)}\sum_{(ij)} 4\cos\left(\mathbf{k}_a.\Delta\mathbf{y}_{ij}\right)\cos\left(\mathbf{k}_b.\Delta\mathbf{y}_{ij}\right). \end{aligned} \tag{A.6}$$

The prefactor 8/9 in this expression is consistent with the factor $F_{\rm corr}^{(2)}(N,m)$, obtained for $N=m=3$ from eq. (3.10).

Case IV concerns diagrams with 3 off-diagonal gluons. Examples for such contributions are depicted in figure 11. If all three gluons are linked to the same pair of sources

JHEP12(2017)074

(see, e.g., figure 11(a)), we find for the symmetrized expression

$$\hat{\sigma}_{IVa}\left(\{\mathbf{k_1},\mathbf{k}_2,\mathbf{k}_3\},\{\mathbf{y}_1,\mathbf{y}_2,\mathbf{y}_3\}\right) \propto (N_c^2-1)^3 N_c^3 \left|\vec{f}(\mathbf{k}_1)\right|^2 \left|\vec{f}(\mathbf{k}_2)\right|^2 \left|\vec{f}(\mathbf{k}_3)\right|^2 \times \frac{1}{4(N_c^2-1)} \sum_{(ij)} 8\cos\left(\mathbf{k}_1.\Delta\mathbf{y}_{ij}\right)\cos\left(\mathbf{k}_2.\Delta\mathbf{y}_{ij}\right)\cos\left(\mathbf{k}_3.\Delta\mathbf{y}_{ij}\right). \tag{A.7}$$

If the 3 off-diagonal gluons are linked to exactly two pairs of sources (see, e.g., figure 11(b)), then one of the color traces vanishes,

$$\hat{\sigma}_{IVb} = 0\,. \tag{A.8}$$

If the three off-diagonal gluons are linked to exactly three pairs of sources (see, e.g., figure 11(c)), one finds

$$M_{IVc}\left(\{\mathbf{k_1},\mathbf{k}_2,\mathbf{k}_3\},\{\mathbf{y}_1,\mathbf{y}_2,\mathbf{y}_3\}\right) \propto (N_c^2-1)^3 N_c^3 \left|\vec{f}(\mathbf{k}_1)\right|^2 \left|\vec{f}(\mathbf{k}_2)\right|^2 \left|\vec{f}(\mathbf{k}_3)\right|^2 \times \frac{1}{(N_c^2-1)^2} \sum_{(a,b,c)} 8\cos\left(\mathbf{k}_a.\Delta\mathbf{y}_{12}\right)\cos\left(\mathbf{k}_b.\Delta\mathbf{y}_{23}\right)\cos\left(\mathbf{k}_c.\Delta\mathbf{y}_{31}\right). \tag{A.9}$$

Parametrically, contributions to (A.9) are suppressed by an extra factor (N_c^2-1) compared to (A.7). The prefactors of these expressions can be understood by noting that contributions to (A.7) (see figure 11(a)) have a color factor

$$\mathrm{Tr}\left[\mathbb{1}\right]\,\mathrm{Tr}\left[T^aT^cT^b\right]\,\mathrm{Tr}\left[T^aT^bT^c\right] = \frac{1}{4}N_c^3(N_c^2-1)^2\,, \tag{A.10}$$

while contributions to (A.9) (see figure 11(c)) have a color trace

$$\mathrm{Tr}\left[T^cT^b\right]\,\mathrm{Tr}\left[T^bT^a\right]\,\mathrm{Tr}\left[T^aT^c\right] = N_c^3(N_c^2-1)\,. \tag{A.11}$$

B Multi-gluon emission for $N = m = 4$

Here, we give details of the calculation of $m = 4$ gluons emitted from $N = 4$ sources. We consider a total of $N^{2m} = 4^8$ diagrams, classified as

I 4 diagonal gluons (4^4 diagrams)

II 3 diagonal gluons and 1 off-diagonal gluon (12×4^4 diagrams)

III 2 diagonal gluons and 2 off-diagonal gluon ($2 \times 3^3 \times 4^4$ diagrams)

IV 1 diagonal gluon and 3 off-diagonal gluons ($4 \times 3^3 \times 4^4$ diagrams)

V 4 off-diagonal gluons ($3^4 \times 4^4$ diagrams)

JHEP12(2017)074

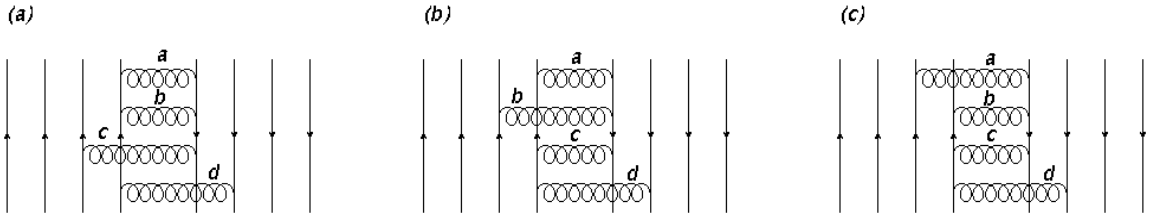

Figure 12. Examples of diagrammatic contributions with 2 off-diagonal and 2 diagonal gluons that are all connected to the same pair of sources. The three diagrams differ by the number of 0, 1 and 2 diagonal gluons placed in between the off-diagonal gluons, and this changes the color trace, see text for details.

The **cases I and II** are trivial: diagrams with only diagonal gluons are counted with color factor $N_c^4(N_c^2-1)^4$ and diagrams with exactly one off-diagonal gluon have a vanishing color trace,

$$\hat{\sigma}_I \propto (N_c^2-1)^4 N_c^4 \left|\vec{f}(\mathbf{k}_1)\right|^2 \left|\vec{f}(\mathbf{k}_2)\right|^2 \left|\vec{f}(\mathbf{k}_3)\right|^2 \left|\vec{f}(\mathbf{k}_4)\right|^2 4^4\,, \tag{B.1}$$

$$\hat{\sigma}_{II} = 0\,. \tag{B.2}$$

For the three other cases, however, qualitatively novel features arise as we discuss now.

Case III includes diagrams with two off-diagonal gluons linked to 2, 3 or 4 sources. Only the first of these possibilities gives non-vanishing contributions. It includes 9×4^4 diagrams. Figure 12 depicts some of them. One checks easily that these contributions have different color traces, namely

$$\mathrm{Tr}\,[\mathbb{1}]\ \mathrm{Tr}\,[\mathbb{1}]\ \mathrm{Tr}[T^aT^bT^cT^dT^bT^a]\,\mathrm{Tr}[T^cT^d] = N_c^4(N_c^2-1)^3\,, \tag{B.3}$$

if in between the off-diagonal exchanges there is no diagonal gluon exchange (see, e.g., figure 12(a)),

$$\mathrm{Tr}\,[\mathbb{1}]\ \mathrm{Tr}\,[\mathbb{1}]\ \mathrm{Tr}[T^aT^bT^cT^dT^cT^a]\,\mathrm{Tr}[T^bT^d] = \frac{1}{2}N_c^4(N_c^2-1)^3\,, \tag{B.4}$$

if one of the two diagonal gluons is exchanged in between the off-diagonal ones (see, e.g., figure 12(b)), and

$$\mathrm{Tr}\,[\mathbb{1}]\ \mathrm{Tr}\,[\mathbb{1}]\ \mathrm{Tr}[T^aT^bT^cT^dT^cT^b]\,\mathrm{Tr}[T^aT^d] = \frac{1}{4}N_c^4(N_c^2-1)^3\,, \tag{B.5}$$

if both diagonal gluon exchanges occur in between the off-diagonal ones (see, e.g., figure 12(c)). This illustrates the general statements about diagonal gluons sandwiched between off-diagonal ones that are made in section 3.2.1.

JHEP12(2017)074

Evaluating these color traces for each of the 9×4^4 diagrams, we find $\Delta\mathbf{y}_{ij}\equiv(\mathbf{y}_i-\mathbf{y}_j)$

$$\begin{aligned}\hat{\sigma}_{III}^{(ord)} \propto (N_c^2-1)^3N_c^4 &\left|\vec{f}(\mathbf{k}_1)\right|^2\left|\vec{f}(\mathbf{k}_2)\right|^2\left|\vec{f}(\mathbf{k}_3)\right|^2\left|\vec{f}(\mathbf{k}_4)\right|^2\ 4\\ \times\Big\{4^2\sum_{(ij)}&[\cos(\mathbf{k}_1.\Delta\mathbf{y}_{ij})\cos(\mathbf{k}_2.\Delta\mathbf{y}_{ij})+\cos(\mathbf{k}_3.\Delta\mathbf{y}_{ij})\cos(\mathbf{k}_4.\Delta\mathbf{y}_{ij})\\ &+\cos(\mathbf{k}_2.\Delta\mathbf{y}_{ij})\cos(\mathbf{k}_3.\Delta\mathbf{y}_{ij})]\\ +3\cdot 4\sum_{(ij)}&[\cos(\mathbf{k}_1.\Delta\mathbf{y}_{ij})\cos(\mathbf{k}_3.\Delta\mathbf{y}_{ij})+\cos(\mathbf{k}_2.\Delta\mathbf{y}_{ij})\cos(\mathbf{k}_4.\Delta\mathbf{y}_{ij})]\\ +9\sum_{(ij)}&\cos(\mathbf{k}_2.\Delta\mathbf{y}_{ij})\cos(\mathbf{k}_3.\Delta\mathbf{y}_{ij})\Big\}\,.\end{aligned}\tag{B.6}$$

The prefactors in this expression follow from considering the 6 choices of distributing two diagonal gluons in an ordered list of four gluons. For three of these choices, the diagonal gluons are not sandwiched between the off-diagonal ones (such, e.g., figure 12(a)) and there are 4^2 possibilities to connect the diagonal gluons to sources. This fixes the prefactor of the first three terms in (B.6). In addition, there are 2 choices, for which one of the two diagonal gluons is sandwiched between the off-diagonal one (see, e.g., figure 12(b)). In this class of diagrams, there are 4×2 diagrams with color trace (B.3) and there are 4×2 diagrams with color trace (B.4). This determines the prefactor in the second line of (B.6), namely $4\times 2+4\times 2\times 1/2=4\times 3$. Finally, one can sandwich both diagonal gluons in between the off-diagonal ones (see, e.g., figure 12(3)). Amongst the 4^2 possibilities of connecting the diagonal gluons to sources, there are then 4 with trace (B.3), there are 8 with trace (B.4) and there are another 4 with trace (B.5), giving the prefactor $4\times 1+8\times 1/2+4\times 1/4=9$ of the last term of (B.6).

Randomizing according to (2.3) over (B.6), we obtain

$$\begin{aligned}\hat{\sigma}_{III} \propto (N_c^2-1)^3N_c^4 &\left|\vec{f}(\mathbf{k}_1)\right|^2\left|\vec{f}(\mathbf{k}_2)\right|^2\left|\vec{f}(\mathbf{k}_3)\right|^2\left|\vec{f}(\mathbf{k}_4)\right|^2\\ \times\frac{27}{32}4^2\sum_{(ab)}\sum_{(ij)}&4\cos(\mathbf{k}_a.\Delta\mathbf{y}_{ij})\cos(\mathbf{k}_b.\Delta\mathbf{y}_{ij})\,.\end{aligned}\tag{B.7}$$

Here, the sum $\sum_{(ab)}$ goes over the $m(m-1)/2=6$ pairs of emitted gluons. The correction factor 27/32 is obtained by pulling the overall factor $4^2m(m-1)/2$ out of each of the terms in (B.6) and summing up the remaining terms $\left(3+2\times 3/4+9/4^2\right)/6=27/32$. This coincides with $F_{\rm corr}^{(2)}(4,4)$, see eq. (3.10).

Case IV contains diagrams in which three off-diagonal gluons

i) are linked to exactly one pair of sources (i,j).

ii) are linked to two pairs of sources (ij), (jl) made of three sources.

iii) are linked to two pairs of sources (ij), (lm) made of four sources.

iv) are linked to three pairs of sources (ij), (jl), (li) made of three sources.

v) are linked to 3 pairs made of four sources.

JHEP12(2017)074

These contributions have i) 3×4^4, ii) 9×4^5, iii) 9×4^4, iv) 3×4^5 and v) 3×4^6 diagramms respectively, that sum up to a total of $3^3\times 4^5$ diagrams. The contributions ii), iii) and v) can be checked easily to have vanishing color traces. The contribution IVi) yields (we present symmetrized cross sections according to (2.3))

$$M_{IVi} \propto \frac{1}{4}N_c^4\,(N_c^2-1)^3\left|\vec{f}(\mathbf{k}_1)\right|^2\left|\vec{f}(\mathbf{k}_2)\right|^2\left|\vec{f}(\mathbf{k}_3)\right|^2\left|\vec{f}(\mathbf{k}_4)\right|^2\frac{7}{8}N \times\sum_{(abc)}\sum_{(lm)}8\cos\left(\mathbf{k}_a.\Delta\mathbf{y}_{lm}\right)\cos\left(\mathbf{k}_b.\Delta\mathbf{y}_{lm}\right)\cos\left(\mathbf{k}_c.\Delta\mathbf{y}_{lm}\right), \tag{B.8}$$

where the sum $\sum_{(abc)}$ runs over the four possibilities of selecting three of four particle momenta in the final state. The color traces of diagrams contributing to (B.8) are $\frac{1}{4}N_c^4\,(N_c^2-1)^3$ if the diagonal gluon is not linked to source l or m, but it is $\frac{1}{8}N_c^4\,(N_c^2-1)^3$ if the diagonal gluon is sandwiched between the off-diagonal ones and linked to l or m. After symmetrization, this smaller color trace of some diagrams leads to a color correction factor 7/8. To keep track of the origin of different factors, we write in (B.8) the factor N for the number of possibilities to link the diagonal gluon to one of the N sources. Compared to (B.1), the contribution (B.8) is $O(N^{-1})$ suppressed.

Similarly, for diagrams contributing to case IViv, we find color traces $N_c^4\,(N_c^2-1)^2$, as well as $\frac{1}{2}N_c^4\,(N_c^2-1)^3$ for some diagrams. After symmetrization, the reduced color trace can be absorbed in a color correction factor 7/8 and one finds

$$M_{IViv} \propto (N_c^2-1)^2N_c^4\left|\vec{f}(\mathbf{k}_1)\right|^2\left|\vec{f}(\mathbf{k}_2)\right|^2\left|\vec{f}(\mathbf{k}_3)\right|^2\left|\vec{f}(\mathbf{k}_4)\right|^2\frac{7}{8}\,N \times\sum_{(abc)}\sum_{(lm)(mn)(nl)}8\cos\left(\mathbf{k}_a.\Delta\mathbf{y}_{lm}\right)\cos\left(\mathbf{k}_b.\Delta\mathbf{y}_{mn}\right)\cos\left(\mathbf{k}_c.\Delta\mathbf{y}_{nl}\right). \tag{B.9}$$

For the prefactors of these expressions, there is the following consistency check: one recalls that each diagram contributes phase factors with prefactor 1 times a color trace. Hence, if one ignores the color correction factor and if one multiplies the 4 terms in the sum $\sum_{(abc)}$ times the $N(N-1)(N-2)$ terms in $\sum_{(lm)(mn)(nl)}$ times the explicit prefactor $N\,8$, the result should match the number 3×4^5 of diagrams contributing to case IViv.

Case V includes diagrams with four off-diagonal gluons that are

i) emitted from two sources, i.e., one pair of sources (i,j).

ii) emitted from three sources that combine to two pairs of sources (lm), (mn).

iii) emitted from three sources that combine to three pairs of sources (lm), (mn), (n,l).

iv) emitted from four sources that combine to two pairs of sources (lm) and (no).

v) emitted from four sources that combine to three pairs of sources (lm), (mn), (no).

vi) emitted from four sources that combine to four pairs of sources (lm), (mn), (no), (ol).

These contributions include i) 6×4^2 ii) $6\times 4^4+2\times 3^2\times 4^3$ iii) $3^2\times 4^4$ iv) $2^5\times 3^2+6\times 4^3$ v) $3^3\times 4^4+3^2\times 4^4$ vi) $2\times 3^2\times 4^3+2\times 3^2\times 4^4$ diagrams, respectively, and they add up to $3^4\times 4^4$ diagrams.

JHEP12(2017)074

Case Vi) comprises diagrams with more complicated color trace

$$\mathrm{Tr}\,[\mathbb{1}]^2\,\mathrm{Tr}\left[T^aT^bT^cT^d\right]\,\mathrm{Tr}\left[T^dT^cT^bT^a\right]=\frac{1}{8}N_c^2\left(N_c^4+11N_c^2-12\right)\left(N_c^2-1\right)^2\,, \tag{B.10}$$

that result in

$$\begin{aligned}M_{Vi}\propto&\,\frac{1}{8}N_c^2\left(N_c^2-1\right)^2\left(N_c^4+11N_c^2-12\right)\left|\vec{f}(\mathbf{k}_1)\right|^2\left|\vec{f}(\mathbf{k}_2)\right|^2\left|\vec{f}(\mathbf{k}_3)\right|^2\left|\vec{f}(\mathbf{k}_4)\right|^2\\&\times\sum_{(lm)}2^4\cos\left(\mathbf{k}_1.\Delta\mathbf{y}_{lm}\right)\cos\left(\mathbf{k}_2.\Delta\mathbf{y}_{lm}\right)\cos\left(\mathbf{k}_3.\Delta\mathbf{y}_{lm}\right)\cos\left(\mathbf{k}_4.\Delta\mathbf{y}_{lm}\right).\end{aligned} \tag{B.11}$$

It is a simple consistency check to test that the number of $N(N-1)/2$ terms in the sum times the prefactor 2^4 matches the number of diagrams in case Vi.

Case Vii) comprises 6×4^4 diagrams for which three off-diagonal gluons are attached to one pair of sources. These diagrams vanish. It also comprises $2\times3^2\times4^3$ diagrams in which two off-diagonal gluons are attached to each pairs of sources. For these latter diagrams, 'most' color traces are $N_c^4\left(N_c^2-1\right)^2$ but 'some' are $\frac{1}{2}N_c^4\left(N_c^2-1\right)^2$. In the symmetrized expression, the modifications due to the smaller color trace can be accounted for by a color correction factor 5/6 and one obtains

$$\begin{aligned}\hat{\sigma}_{Vii1}\propto&\,N_c^4\left(N_c^2-1\right)^2\left|\vec{f}(\mathbf{k}_1)\right|^2\left|\vec{f}(\mathbf{k}_2)\right|^2\left|\vec{f}(\mathbf{k}_3)\right|^2\left|\vec{f}(\mathbf{k}_4)\right|^2\sum_{(lm)(mn)}\\&\times\frac{5}{6}\sum_{(ab),(cd)}2^4\cos\left(\mathbf{k}_a.\Delta\mathbf{y}_{lm}\right)\cos\left(\mathbf{k}_b.\Delta\mathbf{y}_{lm}\right)\cos\left(\mathbf{k}_c.\Delta\mathbf{y}_{mn}\right)\cos\left(\mathbf{k}_d.\Delta\mathbf{y}_{mn}\right).\end{aligned} \tag{B.12}$$

Here, the sum $\sum_{(lm)(mn)}$ goes over the $N(N-1)(N-2)/2=4\times3$ possibilities of picking two pairs of sources that have one source in common. The sum $\sum_{(ab),(cd)}$ goes over the $m(m-1)/2\ (m-2)(m-3)/2=6$ possibilities of picking an ordered list of two pairs. As a consistency check, one can multiply these factors with the explicit prefactor 2^4 in (B.12) to recover the number of $2\times3^2\times4^3$ diagrams of this case.

However, there is an additional contribution to this case in which one finds for the first time sin-terms. This contribution breaks the symmetry $\mathbf{k}_i\to-\mathbf{k}_i$, and can therefore give rise to odd harmonics. It reads

$$\begin{aligned}\hat{\sigma}_{Vii2}^{(ord)}\propto&\,N_c^4\left(N_c^2-1\right)^2\left|\vec{f}(\mathbf{k}_1)\right|^2\left|\vec{f}(\mathbf{k}_2)\right|^2\left|\vec{f}(\mathbf{k}_3)\right|^2\left|\vec{f}(\mathbf{k}_4)\right|^2\\&\times\sum_{(lm)(mn)}\Big\{-4\cos\left(\mathbf{k}_1.\Delta\mathbf{y}_{lm}\right)\sin\left(\mathbf{k}_2.\Delta\mathbf{y}_{mn}\right)\sin\left(\mathbf{k}_3.\Delta\mathbf{y}_{mn}\right)\cos\left(\mathbf{k}_4.\Delta\mathbf{y}_{lm}\right)\\&\quad-4\cos\left(\mathbf{k}_1.\Delta\mathbf{y}_{mn}\right)\sin\left(\mathbf{k}_2.\Delta\mathbf{y}_{lm}\right)\sin\left(\mathbf{k}_3.\Delta\mathbf{y}_{lm}\right)\cos\left(\mathbf{k}_4.\Delta\mathbf{y}_{mn}\right)\\&\quad-4\cos\left(\mathbf{k}_1.\Delta\mathbf{y}_{lm}\right)\sin\left(\mathbf{k}_2.\Delta\mathbf{y}_{mn}\right)\sin\left(\mathbf{k}_3.\Delta\mathbf{y}_{lm}\right)\cos\left(\mathbf{k}_4.\Delta\mathbf{y}_{mn}\right)\\&\quad-4\cos\left(\mathbf{k}_1.\Delta\mathbf{y}_{mn}\right)\sin\left(\mathbf{k}_2.\Delta\mathbf{y}_{lm}\right)\sin\left(\mathbf{k}_3.\Delta\mathbf{y}_{mn}\right)\cos\left(\mathbf{k}_4.\Delta\mathbf{y}_{lm}\right)\Big\}.\end{aligned} \tag{B.13}$$

We write $\hat{\sigma}_{Vii2}^{(ord)}$, without symmetrizing over gluon momenta, for $\mathbf{k}_1,\ldots\mathbf{k}_4$ ordered from top to bottom in emission diagrams. The origin of these sin-terms has been discussed in subsection 5.2.1.

JHEP12(2017)074

In a similar way, one can inspect in detail all diagrams of the case Viii. The result can be expressed again in terms of one contributions with cos-terms only (that we write in symmetrized form) and one contribution that contains sin-terms (and that we write first in un-symmetrized form)

$$M_{Viii1} \propto N_c^4 \left(N_c^2-1\right)^2 \left|\vec{f}(\mathbf{k}_1)\right|^2 \left|\vec{f}(\mathbf{k}_2)\right|^2 \left|\vec{f}(\mathbf{k}_3)\right|^2 \left|\vec{f}(\mathbf{k}_4)\right|^2 \sum_{\underline{(lm)}(mn)(nl)} \tag{B.14}$$

$$\times \frac{1}{24} \sum_{(abcd)} 2^4 \cos\left(\mathbf{k}_a.\Delta\mathbf{y}_{lm}\right)\cos\left(\mathbf{k}_b.\Delta\mathbf{y}_{lm}\right)\cos\left(\mathbf{k}_c.\Delta\mathbf{y}_{mn}\right)\cos\left(\mathbf{k}_d.\Delta\mathbf{y}_{nl}\right),$$

$$\begin{aligned} M_{Viii2}^{(ord)} \propto N_c^4 \left(N_c^2-1\right)^2 & \left|\vec{f}(\mathbf{k}_1)\right|^2 \left|\vec{f}(\mathbf{k}_2)\right|^2 \left|\vec{f}(\mathbf{k}_3)\right|^2 \left|\vec{f}(\mathbf{k}_4)\right|^2 \sum_{\underline{(lm)}(mn)(nl)} \\ \times \Big\{ & -4\cos\left(\mathbf{k}_1.\Delta\mathbf{y}_{lm}\right)\sin\left(\mathbf{k}_2.\Delta\mathbf{y}_{lm}\right)\sin\left(\mathbf{k}_3.\Delta\mathbf{y}_{mn}\right)\cos\left(\mathbf{k}_4.\Delta\mathbf{y}_{nl}\right) \\ & -4\cos\left(\mathbf{k}_1.\Delta\mathbf{y}_{lm}\right)\sin\left(\mathbf{k}_2.\Delta\mathbf{y}_{lm}\right)\sin\left(\mathbf{k}_3.\Delta\mathbf{y}_{nl}\right)\cos\left(\mathbf{k}_4.\Delta\mathbf{y}_{mn}\right) \\ & -4\cos\left(\mathbf{k}_1.\Delta\mathbf{y}_{lm}\right)\sin\left(\mathbf{k}_2.\Delta\mathbf{y}_{mn}\right)\sin\left(\mathbf{k}_3.\Delta\mathbf{y}_{nl}\right)\cos\left(\mathbf{k}_4.\Delta\mathbf{y}_{lm}\right) \\ & -4\cos\left(\mathbf{k}_1.\Delta\mathbf{y}_{lm}\right)\sin\left(\mathbf{k}_2.\Delta\mathbf{y}_{nl}\right)\sin\left(\mathbf{k}_3.\Delta\mathbf{y}_{mn}\right)\cos\left(\mathbf{k}_4.\Delta\mathbf{y}_{lm}\right) \\ & -4\cos\left(\mathbf{k}_1.\Delta\mathbf{y}_{mn}\right)\sin\left(\mathbf{k}_2.\Delta\mathbf{y}_{lm}\right)\sin\left(\mathbf{k}_3.\Delta\mathbf{y}_{lm}\right)\cos\left(\mathbf{k}_4.\Delta\mathbf{y}_{nl}\right) \\ & -4\cos\left(\mathbf{k}_1.\Delta\mathbf{y}_{nl}\right)\sin\left(\mathbf{k}_2.\Delta\mathbf{y}_{lm}\right)\sin\left(\mathbf{k}_3.\Delta\mathbf{y}_{lm}\right)\cos\left(\mathbf{k}_4.\Delta\mathbf{y}_{mn}\right) \\ & -4\cos\left(\mathbf{k}_1.\Delta\mathbf{y}_{mn}\right)\sin\left(\mathbf{k}_2.\Delta\mathbf{y}_{lm}\right)\sin\left(\mathbf{k}_3.\Delta\mathbf{y}_{nl}\right)\cos\left(\mathbf{k}_4.\Delta\mathbf{y}_{lm}\right) \\ & -4\cos\left(\mathbf{k}_1.\Delta\mathbf{y}_{nl}\right)\sin\left(\mathbf{k}_2.\Delta\mathbf{y}_{lm}\right)\sin\left(\mathbf{k}_3.\Delta\mathbf{y}_{mn}\right)\cos\left(\mathbf{k}_4.\Delta\mathbf{y}_{lm}\right) \Big\}. \end{aligned} \tag{B.15}$$

Here, the sum $\sum_{\underline{(lm)}(mn)(nl)}$ goes over triplets of source pairs, of which the source pair (lm) is connected to two off-diagonal gluons.

For the case V iv), we obtain

$$M_{Viv1} \propto N_c^4 \left(N_c^2-1\right)^2 \left|\vec{f}(\mathbf{k}_1)\right|^2 \left|\vec{f}(\mathbf{k}_2)\right|^2 \left|\vec{f}(\mathbf{k}_3)\right|^2 \left|\vec{f}(\mathbf{k}_4)\right|^2 \sum_{(lm)(no)} \tag{B.16}$$

$$\times \sum_{(ab),(cd)} 2^4 \cos\left(\mathbf{k}_a.\Delta\mathbf{y}_{lm}\right)\cos\left(\mathbf{k}_b.\Delta\mathbf{y}_{lm}\right)\cos\left(\mathbf{k}_c.\Delta\mathbf{y}_{no}\right)\cos\left(\mathbf{k}_d.\Delta\mathbf{y}_{no}\right),$$

where the sum $\sum_{(lm)(no)}$ goes over the $N(N-1)(N-2)(N-3)/8$ possibilities of picking two independent pairs of sources.

Finally, there is a non-vanishing contribution for connecting four off-diagonal gluons to 4 different pairs of sources, namely

$$M_{Vvi} \propto N_c^4 \left(N_c^2-1\right) \left|\vec{f}(\mathbf{k}_1)\right|^2 \left|\vec{f}(\mathbf{k}_2)\right|^2 \left|\vec{f}(\mathbf{k}_3)\right|^2 \left|\vec{f}(\mathbf{k}_4)\right|^2 \sum_{(lm)(mn)(no)(ol)} \tag{B.17}$$

$$\times \sum_{(abcd))} 2^4 \cos\left(\mathbf{k}_a.\Delta\mathbf{y}_{lm}\right)\cos\left(\mathbf{k}_b.\Delta\mathbf{y}_{mn}\right)\cos\left(\mathbf{k}_c.\Delta\mathbf{y}_{no}\right)\cos\left(\mathbf{k}_d.\Delta\mathbf{y}_{ol}\right).$$

Compared to (B.16), this is suppressed by another power in $1/(N_c^2-1)$. All other cases vanish.

JHEP12(2017)074

C Color correction factors

In this appendix, we derive the color correction factors entering (4.1). The factor $F^{(2)}_{\text{corr}}$ was derived in section 3.2.1 already.

C.1 $F^{(4i)}_{\text{corr}}(N, m)$

We consider the case of $m-4$ diagonal gluons and of four off-diagonal gluons that form two dipoles (lm), (no) with four different sources. This is case V iv1 in appendix B, which is the leading $O\left(1/(N_c^2-1)^2\right)$ contribution to the 4-particle correlator. There are $\binom{m}{4}$ possibilities to assign the 4 off-diagonal gluons to an ordered list of m gluons. For each assignment, there are

- j_1 diagonal gluons between the first and second off-diagonal gluon.
- j_2 diagonal gluons between the second and third off-diagonal gluon.
- j_3 diagonal gluons between the third and fourth off-diagonal gluon.
- $m-4-j_1-j_2-j_3$ before the first or after the last off-diagonal gluon.

The number of possibilities of distributing these $m-4$ gluons such that an arbitrary number of $j_1+j_2+j_3$ gluons lies between the first and last off-diagonal gluon is

$$\sum_{j_3=0}^{m-4} \sum_{j_2=0}^{m-4-j_3} \sum_{j_1=0}^{m-4-j_2-j_3} (m-3-(j_1+j_2+j_3)) = \binom{m}{4}. \tag{C.1}$$

This is a consistency check of our starting point that will be useful in the following. We also note that the total number of different diagrams (for given sources l, m, n, o) is

$$\mathcal{N} = \binom{m}{4} N^{m-4}. \tag{C.2}$$

The four off-diagonal gluons can be paired into dipoles in three different ways. Denoting the off-diagonal gluons as 1, $\bar{1}$, 2, $\bar{2}$ in a notation that makes their pairing clear, the three different paring are

A. Ordering of off-diagonal gluons: 1, $\bar{1}$, 2, $\bar{2}$

B. Ordering of off-diagonal gluons: 1, 2, $\bar{1}$, $\bar{2}$

C. Ordering of off-diagonal gluons: 1, 2, $\bar{2}$, $\bar{1}$

For case A., there are j_1 diagonal gluons sandwiched between the first dipole pair $1\bar{1}$, and j_3 gluons sandwiched between $2\bar{2}$; j_2 gluons are not sandwiched between any dipole pair. l_1 of the j_1 gluons will be linked to the same source pair (lm) as $1\bar{1}$, and analogously for l_3

out of the j_3 gluons sandwiched between $2\bar{2}$. As each diagonal gluon sandwiched between an off-diagonal pair reduces the color trace and thus the spectrum by a factor 2, we have

$$\begin{aligned} F_{\text{corr}}^{(4i,A)}(N,m) &= \frac{1}{\mathcal{N}} \sum_{j_3=0}^{m-4} \sum_{j_2=0}^{m-4-j_3} \sum_{j_1=0}^{m-4-j_2-j_3} (m-3-(j_1+j_2+j_3))\, N^{m-4-(j_1+j_2+j_3)} \\ &\quad \times \sum_{l_3=0}^{j_3} \sum_{l_1=0}^{j_1} \binom{j_1}{l_1} (N-2)^{j_1-l_1} N^{j_2} \binom{j_3}{l_3} (N-2)^{j_3-l_3} \\ &= \frac{(m-4)!}{m!} \left[-24N^{4-m}(-3+m+3N)(N-1)^{m-1} \right. \\ &\qquad \left. +12N^2 \left(m(m-1)-4mN+6N^2\right) \right] . \end{aligned} \tag{C.3}$$

We note that without the above-mentioned factors 1/2, the terms in (C.3) would be multiplied by factors $2^{l_1+l_3}$, and one would find $F_{\text{corr}}^{(4i,A)}(N,m) = 1$.

For case B., there are again j_1 diagonal gluons sandwiched between the first dipole pair $1\bar{1}$, and j_3 gluons sandwiched between $2\bar{2}$. However, there are now j_2 gluons sandwiched between $1\bar{1}$, and $2\bar{2}$. In this case, there will be l_2 out of j_2 gluons that are linked to the dipole (lm) and there will be $\bar{l}_2$ of the j_2 gluons linked to (no). The corresponding color factor reads

$$\begin{aligned} F_{\text{corr}}^{(4i,B)}(N,m) &= \frac{1}{\mathcal{N}(N,m)} \sum_{j_3=0}^{m-4} \sum_{j_2=0}^{m-4-j_3} \sum_{j_1=0}^{m-4-j_2-j_3} (m-3-(j_1+j_2+j_3)) N^{m-4-(j_1+j_2+j_3)} \\ &\quad \times \sum_{l_3=0}^{j_3} \sum_{\bar{l}_2=0}^{j_2} \sum_{l_2=0}^{j_2-\bar{l}_2} \sum_{l_1=0}^{j_1} \binom{j_1}{l_1} (N-2)^{j_1-l_1} \frac{j_2!\,(N-4)^{j_2-l_2-\bar{l}_2}}{l_2!\bar{l}_2!\,(j_2-l_2-\bar{l}_2)!} \binom{j_3}{l_3} (N-2)^{j_3-l_3} \\ &= \frac{6(2m-5N)N^3}{m(m-1)(m-2)(m-3)} \\ &\quad + \frac{6N^{4-m}\left((N-2)^m + 4(N-1)^{m-1}(N+m-1)\right)}{m(m-1)(m-2)(m-3)} . \end{aligned} \tag{C.4}$$

Case C. gives the same result as case B. The color correction factor $F_{\text{corr}}^{(4)}(N,m)$ in equation (4.1) therefore reads

$$\begin{aligned} F_{\text{corr}}^{(4i)}(N,m) &= \frac{1}{3} F_{\text{corr}}^{(4,A)}(N,m) + \frac{2}{3} F_{\text{corr}}^{(4,B)}(N,m) \\ &= \frac{4(m-4)!}{m!} \left[N^2 \left(m(m-1)-2mN+N^2\right) \right. \\ &\qquad \left. +N^{4-m}\left((N-2)^m - 2(N-1)^{m-1}(N-m-1)\right) \right] . \end{aligned} \tag{C.5}$$

Fixing the average number of gluons emitted per source to $\overline{m} = m/N$, we arrive at a compact expression in the high multiplicity limit,

$$\lim_{m\to\infty} F_{\text{corr}}^{(4i)}(m/\overline{m},m) = \left(\frac{2e^{-\overline{m}} + 2\overline{m} - 2}{\overline{m}^2} \right)^2 . \tag{C.6}$$

JHEP12(2017)074

C.2 $F^{(3i)}_{\rm corr}(N,m)$

We consider the case of $m-3$ diagonal gluons and of three off-diagonal gluons that are linked between the source pairs (lm), (mn) and (nl). In close analogy to appendix C.1, we denote by j_1 (j_2) the number of diagonal gluons between the first and second (the second and third) off-diagonal gluon. One checks easily for each of the j_1 diagonal gluons: their color trace is N_c if they link to a source other than l, m or n. Also for exactly one of the three sources l, m, n, the color trace is N_c, but it is $N_c/2$ for the other two sources. Paralleling the logic that lead to (C.3), we therefore find the norm

$$\mathcal{N} = \binom{m}{3} N^{m-3}\,, \tag{C.7}$$

and

$$\begin{aligned} F^{(3i)}_{\rm corr}(N,m) &= \frac{1}{\mathcal{N}} \sum_{j_2=0}^{m-3} \sum_{j_1=0}^{m-3-j_2} \left(m-2-(j_1+j_2)\right) N^{m-3-(j_1+j_2)} \\ &\quad \times \sum_{l_1=0}^{j_1} \sum_{\bar{l}_1=0}^{j_1-l_1} \frac{j_1!}{l_1!\,\bar{l}_1!\,\left(j_1-l_1-\bar{l}_1\right)!} 1^{\bar{l}_1}\, 2^{l_1}\, (N-3)^{j_1-l_1-\bar{l}_1} \\ &\quad \times \sum_{l_2=0}^{j_2} \sum_{\bar{l}_2=0}^{j_2-l_2} \frac{j_2!}{l_2!\,\bar{l}_2!\,\left(j_2-l_2-\bar{l}_2\right)!} 1^{\bar{l}_2}\, 2^{l_2}\, (N-3)^{j_2-l_2-\bar{l}_2} \\ &= \frac{(m-3)!}{m!} \left[6(m-2N)N^2 + 6(N-1)^{m-1} N^{3-m}(-2+m+2N)\right]\,. \end{aligned} \tag{C.8}$$

For $N=m=4$, we find $F^{(3i)}_{\rm corr}(4,4) = \frac{7}{8}$, which is consistent with the explicit calculation in appendix B. The limiting value is

$$\lim_{m\to\infty} F^{(3i)}_{\rm corr}(m/\overline{m},m) = \frac{6e^{-\overline{m}}}{\overline{m}^3}\,(2+\overline{m}) + \frac{6}{\overline{m}^3}\,(\overline{m}-2)\,. \tag{C.9}$$

C.3 $F^{(4ii)}_{\rm corr}(N,m)$

We consider the case of $m-4$ diagonal gluons and of four off-diagonal gluons that are linked between the source pairs (lm), (mn), (no) and (ol). We denote by j_1, j_2 and j_3 the number of diagonal gluons that are sandwiched between the first and second, the second and third and the third and fourth off-diagonal gluon, respectively. One checks easily that each of these diagonal gluons contributes to a color trace with factor N_c if linked to any source other than l, m, n or o. Amongst the sources l, m, n and o, there are always exactly two sources where the color trace is N_c, while the color trace for the two other sources is

JHEP12(2017)074

$N_c/2$. Paralleling the logic of appendices C.1 and C.2, we find

$$
\begin{aligned}
F_{\text{corr}}^{(4ii)}(N,m) &= \frac{1}{\mathcal{N}(N,m)} \sum_{j_3=0}^{m-4} \sum_{j_2=0}^{m-4-j_3} \sum_{j_1=0}^{m-4-j_2-j_3} \left(m-3-(j_1+j_2+j_3)\right) N^{m-4-(j_1+j_2+j_3)} \\
&\quad \times \prod_{i=1}^{3} \left(\sum_{l_i=0}^{j_i} \sum_{\bar{l}_i=0}^{j_i-l_i} \frac{j_i!}{l_i!\,\bar{l}_i!\,\left(j_i-l_i-\bar{l}_i\right)!} 2^{l_i} 2^{\bar{l}_i} \left(N-2\right)^{j_i-l_i-\bar{l}_i} \frac{1}{2^{l_i}} \right) \qquad \text{(C.10)} \\
&= \frac{4!\,(m-4)!}{m!} \Bigg[(m-3N)N^3 \\
&\qquad + \frac{1}{2}(N-1)^{m-2} N^{4-m} \left(m^2 + 6(N-1)^2 + m(-5+4N)\right) \Bigg] .
\end{aligned}
$$

The limiting value is

$$
\lim_{m\to\infty} F_{\text{corr}}^{(4ii)}(m/\overline{m},m) = \frac{e^{-2\overline{m}} \left(9 + 12\overline{m} + 6\overline{m}^2 + e^{2\overline{m}} \left(-9 + 6\overline{m}\right)\right)}{2\overline{m}^4} . \qquad \text{(C.11)}
$$

C.4 $F_{\text{corr}}^{(5)}(N,m)$, $F_{\text{corr}}^{(6)}(N,m)$

The complexity of the combinatorics increases if one considers diagonal gluons linked into diagrams with 5 or 6 off-diagonal gluons. For the terms $F_{\text{corr}}^{(5)}(N,m)$ and $F_{\text{corr}}^{(6)}(N,m)$ in (4.1), however, results can be obtained in close parallel to the derivations given in appendices C.1, C.2 and C.3. We find

$$
\lim_{m\to\infty} F_{\text{corr}}^{(5)}(m/\overline{m},m) = \frac{12\, e^{-2\overline{m}} \left(2 + \overline{m} + e^{2\overline{m}} \left(2 - 3\overline{m} + \overline{m}^2\right) + e^{\overline{m}} \left(-4 + 2\overline{m} + \overline{m}^2\right)\right)}{\overline{m}^5} , \qquad \text{(C.12)}
$$

and

$$
\lim_{m\to\infty} F_{\text{corr}}^{(6)}(m/\overline{m},m) = \frac{8\, e^{-3\overline{m}} \left(1 + e^{\overline{m}} \left(-1 + \overline{m}\right)\right)^3}{\overline{m}^6} . \qquad \text{(C.13)}
$$

References

[1] T. Sjöstrand, *The development of MPI modelling in PYTHIA*, arXiv:1706.02166 [INSPIRE].

[2] S. Gieseke, M.H. Seymour and A. Siodmok, *A model of non-perturbative gluon emission in an initial state parton shower*, *JHEP* **06** (2008) 001 [arXiv:0712.1199] [INSPIRE].

[3] S. Gieseke, P. Kirchgaeßer and F. Loshaj, *Soft interactions in HERWIG*, arXiv:1703.10808 [INSPIRE].

[4] SHERPA collaboration, H. Schulz, *SHRiMPS — status of soft interactions in SHERPA*, in *Proceedings of the Seventh International Workshop on Multiple Partonic Interactions at the Large Hadron Collider*, http://indico.ictp.it/event/a14280/, Trieste Italy, 23–27 November 2015 [INSPIRE].

[5] CMS collaboration, *Jet momentum dependence of jet quenching in PbPb collisions at* $\sqrt{s_{NN}} = 2.76$ *TeV*, *Phys. Lett.* **B 712** (2012) 176 [arXiv:1202.5022] [INSPIRE].

JHEP12(2017)074

[6] ATLAS collaboration, *Measurements of the nuclear modification factor for jets in Pb+Pb collisions at* $\sqrt{s_{NN}} = 2.76$ *TeV with the ATLAS detector*, *Phys. Rev. Lett.* **114** (2015) 072302 [arXiv:1411.2357] [INSPIRE].

[7] ALICE collaboration, *Measurement of charged jet suppression in Pb-Pb collisions at* $\sqrt{s_{NN}} = 2.76$ *TeV*, *JHEP* **03** (2014) 013 [arXiv:1311.0633] [INSPIRE].

[8] A. Kurkela, *Initial state of heavy-ion collisions: isotropization and thermalization*, *Nucl. Phys.* **A 956** (2016) 136 [arXiv:1601.03283] [INSPIRE].

[9] U. Heinz and R. Snellings, *Collective flow and viscosity in relativistic heavy-ion collisions*, *Ann. Rev. Nucl. Part. Sci.* **63** (2013) 123 [arXiv:1301.2826] [INSPIRE].

[10] ALICE collaboration, *Enhanced production of multi-strange hadrons in high-multiplicity proton-proton collisions*, *Nature Phys.* **13** (2017) 535 [arXiv:1606.07424] [INSPIRE].

[11] CMS collaboration, *Evidence for collective multiparticle correlations in p-Pb collisions*, *Phys. Rev. Lett.* **115** (2015) 012301 [arXiv:1502.05382] [INSPIRE].

[12] CMS collaboration, *Evidence for collectivity in pp collisions at the LHC*, *Phys. Lett.* **B 765** (2017) 193 [arXiv:1606.06198] [INSPIRE].

[13] ATLAS collaboration, *Measurement of multi-particle azimuthal correlations in pp, p+Pb and low-multiplicity Pb+Pb collisions with the ATLAS detector*, *Eur. Phys. J.* **C 77** (2017) 428 [arXiv:1705.04176] [INSPIRE].

[14] ATLAS collaboration, *Observation of long-range elliptic azimuthal anisotropies in* $\sqrt{s} = 13$ *and 2.76 TeV pp collisions with the ATLAS detector*, *Phys. Rev. Lett.* **116** (2016) 172301 [arXiv:1509.04776] [INSPIRE].

[15] N. Fischer and T. Sjöstrand, *Thermodynamical string fragmentation*, *JHEP* **01** (2017) 140 [arXiv:1610.09818] [INSPIRE].

[16] P. Bozek, *Collective flow in p-Pb and d-Pd collisions at TeV energies*, *Phys. Rev.* **C 85** (2012) 014911 [arXiv:1112.0915] [INSPIRE].

[17] A. Bzdak, B. Schenke, P. Tribedy and R. Venugopalan, *Initial state geometry and the role of hydrodynamics in proton-proton, proton-nucleus and deuteron-nucleus collisions*, *Phys. Rev.* **C 87** (2013) 064906 [arXiv:1304.3403] [INSPIRE].

[18] L. He, T. Edmonds, Z.-W. Lin, F. Liu, D. Molnar and F. Wang, *Anisotropic parton escape is the dominant source of azimuthal anisotropy in transport models*, *Phys. Lett.* **B 753** (2016) 506 [arXiv:1502.05572] [INSPIRE].

[19] ALICE collaboration, *Measurement of charged jet production cross sections and nuclear modification in p-Pb collisions at* $\sqrt{s_{NN}} = 5.02$ *TeV*, *Phys. Lett.* **B 749** (2015) 68 [arXiv:1503.00681] [INSPIRE].

[20] ATLAS collaboration, *Centrality and rapidity dependence of inclusive jet production in* $\sqrt{s_{NN}} = 5.02$ *TeV proton-lead collisions with the ATLAS detector*, *Phys. Lett.* **B 748** (2015) 392 [arXiv:1412.4092] [INSPIRE].

[21] CMS collaboration, *Measurement of inclusive jet production and nuclear modifications in pPb collisions at* $\sqrt{s_{NN}} = 5.02$ *TeV*, *Eur. Phys. J.* **C 76** (2016) 372 [arXiv:1601.02001] [INSPIRE].

[22] N. Borghini, P.M. Dinh and J.-Y. Ollitrault, *A new method for measuring azimuthal distributions in nucleus-nucleus collisions*, *Phys. Rev.* **C 63** (2001) 054906 [nucl-th/0007063] [INSPIRE].

JHEP12(2017)074

[23] N. Borghini, P.M. Dinh and J.-Y. Ollitrault, *Flow analysis from multiparticle azimuthal correlations*, *Phys. Rev.* **C 64** (2001) 054901 [nucl-th/0105040] [INSPIRE].

[24] A. Bilandzic, R. Snellings and S. Voloshin, *Flow analysis with cumulants: direct calculations*, *Phys. Rev.* **C 83** (2011) 044913 [arXiv:1010.0233] [INSPIRE].

[25] T. Altinoluk, N. Armesto, G. Beuf, A. Kovner and M. Lublinsky, *Bose enhancement and the ridge*, *Phys. Lett.* **B 751** (2015) 448 [arXiv:1503.07126] [INSPIRE].

[26] T. Altinoluk, N. Armesto, G. Beuf, A. Kovner and M. Lublinsky, *Hanbury-Brown-Twiss measurements at large rapidity separations, or can we measure the proton radius in p-A collisions?*, *Phys. Lett.* **B 752** (2016) 113 [arXiv:1509.03223] [INSPIRE].

[27] T. Lappi, B. Schenke, S. Schlichting and R. Venugopalan, *Tracing the origin of azimuthal gluon correlations in the color glass condensate*, *JHEP* **01** (2016) 061 [arXiv:1509.03499] [INSPIRE].

[28] A. Dumitru, L. McLerran and V. Skokov, *Azimuthal asymmetries and the emergence of "collectivity" from multi-particle correlations in high-energy pA collisions*, *Phys. Lett.* **B 743** (2015) 134 [arXiv:1410.4844] [INSPIRE].

[29] A. Kovner, M. Lublinsky and V. Skokov, *Exploring correlations in the CGC wave function: odd azimuthal anisotropy*, *Phys. Rev.* **D 96** (2017) 016010 [arXiv:1612.07790] [INSPIRE].

[30] A. Dumitru, K. Dusling, F. Gelis, J. Jalilian-Marian, T. Lappi and R. Venugopalan, *The ridge in proton-proton collisions at the LHC*, *Phys. Lett.* **B 697** (2011) 21 [arXiv:1009.5295] [INSPIRE].

[31] E. Levin and A.H. Rezaeian, *The ridge from the BFKL evolution and beyond*, *Phys. Rev.* **D 84** (2011) 034031 [arXiv:1105.3275] [INSPIRE].

[32] A. Kovner and M. Lublinsky, *Angular correlations in gluon production at high energy*, *Phys. Rev.* **D 83** (2011) 034017 [arXiv:1012.3398] [INSPIRE].

[33] A. Kovner and M. Lublinsky, *On angular correlations and high energy evolution*, *Phys. Rev.* **D 84** (2011) 094011 [arXiv:1109.0347] [INSPIRE].

[34] Y.V. Kovchegov and D.E. Wertepny, *Long-range rapidity correlations in heavy-light ion collisions*, *Nucl. Phys.* **A 906** (2013) 50 [arXiv:1212.1195] [INSPIRE].

[35] A. Dumitru and A.V. Giannini, *Initial state angular asymmetries in high energy p+A collisions: spontaneous breaking of rotational symmetry by a color electric field and C-odd fluctuations*, *Nucl. Phys.* **A 933** (2015) 212 [arXiv:1406.5781] [INSPIRE].

[36] K. Dusling and R. Venugopalan, *Azimuthal collimation of long range rapidity correlations by strong color fields in high multiplicity hadron-hadron collisions*, *Phys. Rev. Lett.* **108** (2012) 262001 [arXiv:1201.2658] [INSPIRE].

[37] E. Gotsman, E. Levin and U. Maor, *CGC/saturation approach for high energy soft interactions: 'soft' pomeron structure and v_n in hadron and nucleus collisions from Bose-Einstein correlations*, *Eur. Phys. J.* **C 76** (2016) 607 [arXiv:1607.00594] [INSPIRE].

[38] E. Gotsman, E. Levin and U. Maor, *Bose-Einstein correlations and v_{2n} and v_{2n-1} in hadron and nucleus collisions*, *Phys. Rev.* **D 95** (2017) 034005 [arXiv:1604.04461] [INSPIRE].

[39] L. McLerran and V. Skokov, *Finite numbers of sources, particle correlations and the color glass condensate*, *Nucl. Phys.* **A 947** (2016) 142 [arXiv:1510.08072] [INSPIRE].

[40] G.P. Salam, *Soft emissions and the equivalence of BFKL and CCFM final states*, *JHEP* **03** (1999) 009 [hep-ph/9902324] [INSPIRE].

JHEP12(2017)074

[41] M. Yu. Azarkin, I.M. Dremin and M. Strikman, *Jets in multiparticle production in and beyond geometry of proton-proton collisions at the LHC*, *Phys. Lett.* **B 735** (2014) 244 [arXiv:1401.1973] [INSPIRE].

[42] N. Paver and D. Treleani, *Multi-quark scattering and large p_T jet production in hadronic collisions*, *Nuovo Cim.* **A 70** (1982) 215 [INSPIRE].

[43] M. Mekhfi, *Multiparton processes: an application to double Drell-Yan*, *Phys. Rev.* **D 32** (1985) 2371 [INSPIRE].

[44] J.R. Gaunt and W.J. Stirling, *Double parton distributions incorporating perturbative QCD evolution and momentum and quark number sum rules*, *JHEP* **03** (2010) 005 [arXiv:0910.4347] [INSPIRE].

[45] J.R. Gaunt, C.-H. Kom, A. Kulesza and W.J. Stirling, *Same-sign W pair production as a probe of double parton scattering at the LHC*, *Eur. Phys. J.* **C 69** (2010) 53 [arXiv:1003.3953] [INSPIRE].

[46] B. Blok, Yu. Dokshitzer, L. Frankfurt and M. Strikman, *The four jet production at LHC and Tevatron in QCD*, *Phys. Rev.* **D 83** (2011) 071501 [arXiv:1009.2714] [INSPIRE].

[47] J.R. Gaunt and W.J. Stirling, *Double parton scattering singularity in one-loop integrals*, *JHEP* **06** (2011) 048 [arXiv:1103.1888] [INSPIRE].

[48] B. Blok, Yu. Dokshitser, L. Frankfurt and M. Strikman, *pQCD physics of multiparton interactions*, *Eur. Phys. J.* **C 72** (2012) 1963 [arXiv:1106.5533] [INSPIRE].

[49] M. Diehl, D. Ostermeier and A. Schafer, *Elements of a theory for multiparton interactions in QCD*, *JHEP* **03** (2012) 089 [*Erratum ibid.* **03** (2016) 001] [arXiv:1111.0910] [INSPIRE].

[50] B. Blok, Yu. Dokshitzer, L. Frankfurt and M. Strikman, *Perturbative QCD correlations in multi-parton collisions*, *Eur. Phys. J.* **C 74** (2014) 2926 [arXiv:1306.3763] [INSPIRE].

[51] J.R. Gaunt, R. Maciula and A. Szczurek, *Conventional versus single-ladder-splitting contributions to double parton scattering production of two quarkonia, two Higgs bosons and $c\bar{c}c\bar{c}$*, *Phys. Rev.* **D 90** (2014) 054017 [arXiv:1407.5821] [INSPIRE].

[52] K. Golec-Biernat and E. Lewandowska, *Electroweak boson production in double parton scattering*, *Phys. Rev.* **D 90** (2014) 094032 [arXiv:1407.4038] [INSPIRE].

[53] *Proceedings of the Seventh International Workshop on Multiple Partonic Interactions at the Large Hadron Collider*, http://indico.ictp.it/event/a14280/, Trieste Italy, 23–27 November 2015.

[54] L. Frankfurt and M. Strikman, *Two gluon form-factor of the nucleon and J/ψ photoproduction*, *Phys. Rev.* **D 66** (2002) 031502 [hep-ph/0205223] [INSPIRE].

[55] L. Frankfurt, M. Strikman and C. Weiss, *Dijet production as a centrality trigger for pp collisions at CERN LHC*, *Phys. Rev.* **D 69** (2004) 114010 [hep-ph/0311231] [INSPIRE].

[56] L. Frankfurt, M. Strikman and C. Weiss, *Transverse nucleon structure and diagnostics of hard parton-parton processes at LHC*, *Phys. Rev.* **D 83** (2011) 054012 [arXiv:1009.2559] [INSPIRE].

[57] J. Kuechler, *Measurements of particle production, underlying event and double parton interactions at the LHC*, PoS(LHCP2016)133 [INSPIRE].

[58] ATLAS collaboration, *Study of hard double-parton scattering in four-jet events in pp collisions at $\sqrt{s} = 7$ TeV with the ATLAS experiment*, *JHEP* **11** (2016) 110 [arXiv:1608.01857] [INSPIRE].

JHEP12(2017)074

[59] P. Gunnellini, *Study of high p_T particle production from double parton scatterings at the CMS experiment*, in *Proceedings of the Seventh International Workshop on Multiple Partonic Interactions at the Large Hadron Collider*, http://indico.ictp.it/event/a14280/, Trieste Italy, 23–27 November 2015 [INSPIRE].

[60] CDF collaboration, F. Abe et al., *Measurement of double parton scattering in $\bar{p}p$ collisions at $\sqrt{s} = 1.8$ TeV*, *Phys. Rev. Lett.* **79** (1997) 584 [INSPIRE].

[61] B. Blok and M. Strikman, *Interplay of soft and perturbative correlations in multiparton interactions at central rapidities*, *Phys. Lett.* **B 772** (2017) 219 [arXiv:1611.03649] [INSPIRE].

[62] CMS collaboration, *Evidence for transverse momentum and pseudorapidity dependent event plane fluctuations in PbPb and pPb collisions*, *Phys. Rev.* **C 92** (2015) 034911 [arXiv:1503.01692] [INSPIRE].

[63] C. Shen, Z. Qiu and U. Heinz, *Shape and flow fluctuations in ultracentral Pb+Pb collisions at the energies available at the CERN Large Hadron Collider*, *Phys. Rev.* **C 92** (2015) 014901 [arXiv:1502.04636] [INSPIRE].

[64] F.G. Gardim, F. Grassi, M. Luzum and J.-Y. Ollitrault, *Breaking of factorization of two-particle correlations in hydrodynamics*, *Phys. Rev.* **C 87** (2013) 031901 [arXiv:1211.0989] [INSPIRE].

[65] L. Yan and J.-Y. Ollitrault, *ν_4, ν_5, ν_6, ν_7: nonlinear hydrodynamic response versus LHC data*, *Phys. Lett.* **B 744** (2015) 82 [arXiv:1502.02502] [INSPIRE].

[66] D. Teaney and L. Yan, *Non linearities in the harmonic spectrum of heavy ion collisions with ideal and viscous hydrodynamics*, *Phys. Rev.* **C 86** (2012) 044908 [arXiv:1206.1905] [INSPIRE].

[67] S. Floerchinger, U.A. Wiedemann, A. Beraudo, L. Del Zanna, G. Inghirami and V. Rolando, *How (non-)linear is the hydrodynamics of heavy ion collisions?*, *Phys. Lett.* **B 735** (2014) 305 [arXiv:1312.5482] [INSPIRE].

[68] N. Borghini and J.-Y. Ollitrault, *Momentum spectra, anisotropic flow and ideal fluids*, *Phys. Lett.* **B 642** (2006) 227 [nucl-th/0506045] [INSPIRE].

[69] M. Gyulassy, P. Levai, I. Vitev and T.S. Biro, *Non-Abelian bremsstrahlung and azimuthal asymmetries in high energy p+A reactions*, *Phys. Rev.* **D 90** (2014) 054025 [arXiv:1405.7825] [INSPIRE].

[70] C. Bierlich, G. Gustafson, L. Lönnblad and A. Tarasov, *Effects of overlapping strings in pp collisions*, *JHEP* **03** (2015) 148 [arXiv:1412.6259] [INSPIRE].

[71] C. Bierlich, G. Gustafson and L. Lönnblad, *A shoving model for collectivity in hadronic collisions*, arXiv:1612.05132 [INSPIRE].

[72] C. Bierlich, G. Gustafson and L. Lönnblad, *Collectivity without plasma in hadronic collisions*, arXiv:1710.09725 [INSPIRE].

[73] M.A. Braun, C. Pajares and V.V. Vechernin, *Anisotropic flows from colour strings: Monte-Carlo simulations*, *Nucl. Phys.* **A 906** (2013) 14 [arXiv:1204.5829] [INSPIRE].

[74] V.A. Abramovsky and O.V. Kancheli, *Distribution of secondary hadron multiplicity* (in Russian), *Pisma Zh. Eksp. Teor. Fiz.* **31** (1980) 566 [INSPIRE].

[75] V.A. Abramovsky, E.V. Gedalin, E.G. Gurvich and O.V. Kancheli, *Long range azimuthal correlations in multiple production processes at high-energies*, *JETP Lett.* **47** (1988) 337 [*Pisma Zh. Eksp. Teor. Fiz.* **47** (1988) 281] [INSPIRE].

JHEP12(2017)074